universität wien

MASTERARBEIT / MASTER'S THESIS

Titel der Masterarbeit / Title of the Master's Thesis

„You accumulate what you exudate:

Ultramafic soil characteristics and rhizosphere processes affecting Ni hyperaccumulation of *Odontarrhena chalcidica*"

verfasst von / submitted by

Sören Benedikt Leonard Risse, B.Sc.

angestrebter akademischer Grad / in partial fulfilment of the requirements for the degree of

Master of Science (MSc)

Wien, 2022 / Vienna 2022

Studienkennzahl lt. Studienblatt / degree programme code as it appears on the student record sheet:	UA 066 299
Studienrichtung lt. Studienblatt / degree programme as it appears on the student record sheet:	Interdisziplinäres Masterstudium Environmental Sciences
Betreut von / Supervisor:	Univ.-Prof. Dipl.-Geol. Dr. Stephan Krämer

UNIVERSITÄT FÜR BODENKULTUR WIEN
University of Natural Resources
and Life Sciences, Vienna

This thesis was done in close cooperation with the Institute of Soil Research, Rhizosphere Ecology and Biogeochemistry Group (RHIZO), BOKU, UFT Tulln

Under excellent supervision of:

Priv.-Doz. Dr. Markus Puschenreiter
Institute of Soil Research (IBF)
Department of Forest- and Soil Sciences

&

Dr. Alice Tognacchini
Institute of Soil Research (IBF)
Department of Forest- and Soil Sciences

Acknowledgements

This thesis has only come about through the help of many remarkable people and it is very important to me to express my gratitude to them. First of all, I would like to thank Stephan Krämer for his supervision and support of the chosen topic and for all helpful suggestions throughout the process and especially during the completion of the thesis. Christian Benold is sincerely thanked for his help in the field and for providing the mobile XRF device. I thank Aida Bani for providing the seeds of *Odontarrhena chalcidica* from Albania. Special thanks to Markus Puschenreiter for being open to cooperate with Uni Vienna, for providing the topic and for the warm welcome into the RHIZO group. Many discussions and enlightening conversations have brought me a lot further professionally and personally. For Alice Tognacchini a heartfelt thank you for the great guidance and endless patience during the plant experiment, in the lab and in writing the thesis. Whenever I got stuck, the right advice was always there! I felt right at home as part of the RHIZO working group, which made my time there a wonderful experience.

Table of Content

1 Abstract

Nickel hyperaccumulation is a rare phenomenon whereby plants accumulate Ni in aboveground biomass exceeding concentrations of 1000 μg g^{-1} in dry weight. Hyperaccumulator plants targeting Ni commonly occur on ultramafic soils, which are characterised by low nutrient and extreme concentrations of certain metals such as Ni, Cr and Co. The trait of hyperaccumulation makes these plants particularly good candidates for phytomining, in which hyperaccumulators are planted to extract metals from soils and recover them from biomass, thus providing an alternative to conventional mining. However, it remains unclear how hyperaccumulator plants mobilise great amounts of Ni in soils and which role root exudation plays in this regard. Especially the biogeochemistry of Fe, P and Ni is assumed to be tightly linked in ultramafic soils since Fe oxides are important Ni and P bearing phases.

To investigate the influence of labile and total Ni concentrations in ultramafic soils upon Ni hyperaccumulator plant responses, a gradient of six soils with pseudo-total Ni concentrations ranging from 552 to 1465 mg kg^{-1} and labile (DTPA-extractable) Ni from 41.6 to 158 mg kg^{-1} was created by soil mixing and compared to an additional high pseudo-total (1613 mg kg^{-1}) but low labile (53.1 mg kg^{-1}) Ni soil. The Ni hyperaccumulator *Odontarrhena chalcidica* was grown for 71 days in pots and pore water sampled four times during the experiment to monitor changes in soil solution ionome, pH and dissolved organic carbon (DOC) content. Labile Ni and Fe fractions (DTPA- and $Sr(NO_3)_2$-extractable) as well as P bioavailability were determined before and after the experiment to investigate plant-induced changes.

Results showed that pore water Ni and Fe concentrations were significantly increased by *O. chalcidica* as well as DOC concentrations, pore water and soil pH compared to unplanted soils. The increase of DOC concentrations in pore water were the first indications of root exudation for *O. chalcidica* and presumably the reason for enhanced Ni and Fe solubilisation. Labile Ni (DTPA- and $Sr(NO_3)_2$-extractable) was decreased as a result of excessive plant uptake of the labile fraction and perhaps a reduction due to soil alkalinisation. A positive correlation between Ni in shoots and pseudo-total concentrations in soil was observed , although plant Ni concentrations did not clearly show the same linear pattern of an increase as soil Ni. No significant correlations of plant Ni and labile Ni could be detected and different methods of assessing Ni availability for hyperaccumulator plants were discussed.

2 Zusammenfassung

Nickel-Hyperakkumulation ist ein seltenes Phänomen, bei dem Pflanzen Ni in der oberirdischen Biomasse akkumulieren und dabei Konzentrationen von 1000 μg g^{-1} im Trockengewicht

überschreiten. Nickel-Hyperakkumulatoren, kommen häufig auf ultramafischen Böden vor, die durch niedrigen Gehalt an Nährstoffen, sowie extreme Konzentrationen bestimmter Metalle wie Ni, Cr und Co gekennzeichnet sind. Die Eigenschaft der Hyperakkumulation macht diese Pflanzen zu besonders guten Kandidaten für das Phytomining, bei dem Hyperakkumulatoren angepflanzt werden, um Metalle aus Böden zu extrahieren und aus der Biomasse zurückzugewinnen, um eine Alternative zu konventionellem Gewinn von Metallen darzubieten. Es ist jedoch nach wie vor unklar, wie Hyperakkumulator-Pflanzen große Mengen an Ni in Böden mobilisieren und welche Rolle Wurzelexudate in diesem Zusammenhang spielen. Es wird angenommen, dass die Biogeochemie von Fe, P und Ni in ultramafischen Böden eng miteinander verbunden ist, da Eisenoxide wichtige Ni- und P-haltige Mineralphasen sind.
Um den Einfluss von labilen und Gesamt-Ni-Konzentrationen in ultramafischen Böden auf die Reaktionen von Ni-Hyperakkumulator-Pflanzen zu untersuchen, wurde ein Gradient von sechs Böden mit Gesamt-Ni-Konzentrationen von 552 bis 1465 mg kg^{-1} und labilem (DTPA-extrahierbarem) Ni von 41,6 bis 158 mg kg^{-1} durch Bodenmischung erzeugt und mit einem zusätzlichen Boden mit hohem Gesamt-Ni Gehalt (1613 mg kg^{-1}), aber niedrigem labilem Ni (53,1 mg kg^{-1}) verglichen. Der Ni-Hyperakkumulator *Odontarrhena chalcidica* wurde 71 Tage lang in Pflanztöpfen angebaut und währenddessen viermal Porenwasserproben entnommen, um Veränderungen des Ionoms der Bodenlösung, des pH-Werts und des Gehalts an gelöstem organischem Kohlenstoff (DOC) zu untersuchen. Labile Ni- und Fe-Fraktionen (DTPA- und $Sr(NO_3)_2$-extrahierbar) sowie die Bioverfügbarkeit von P wurden vor und nach dem Experiment bestimmt, um pflanzeninduzierte Veränderungen zu untersuchen.
Die Ergebnisse zeigten, dass die Ni- und Fe-Konzentrationen im Porenwasser durch *O. chalcidica* signifikant erhöht wurden, ebenso wie die DOC-Konzentrationen, das Porenwasser und der pH-Wert des Bodens im Vergleich zu nicht bepflanzten Böden. Der Anstieg der DOC-Konzentrationen im Porenwasser waren die ersten Anzeichen für die Wurzelexsudation von *O. chalcidica* bisher und vermutlich der Grund für die verstärkte Freisetzung von Ni und Fe. Der Gehalt an labilem Ni (DTPA- und $Sr(NO_3)_2$-extrahierbar) nahm ab, was auf eine übermäßige Aufnahme der labilen Fraktion durch die Pflanzen und möglicherweise auf eine Verringerung durch die Alkalisierung des Boden-pHs zurückzuführen ist. Es wurde eine positive Korrelation zwischen den Ni-Konzentrationen in den Sprossen und den Pseudo-Gesamtkonzentrationen im Boden beobachtet, obwohl die Ni-Konzentrationen in den Pflanzen nicht eindeutig das gleiche lineare Muster eines Anstiegs aufwiesen wie der Ni Gesamtgehalt im Boden. Es konnten keine signifikanten Korrelationen zwischen pflanzlichem Ni und labilem Ni festgestellt werden, und es wurden verschiedene Methoden zur Bewertung der Ni-Verfügbarkeit für hyperakkumulierende Pflanzen diskutiert.

3 Graphical abstract

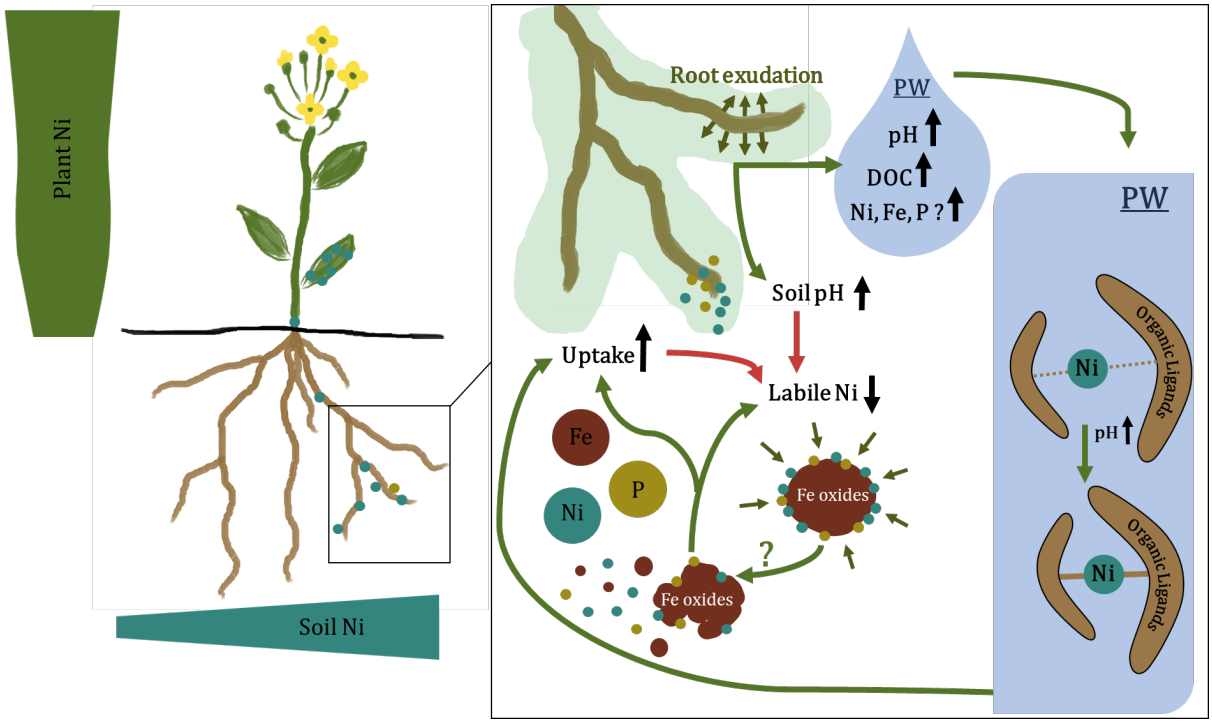

Figure 1 Graphical abstract: An overview of the observed results of the pot experiment, green arrows illustrate a process resulting in an increase, red arrows in a decrease. First indicators of root exudation for O. chalcidica *have been made by increased DOC concentrations in pore water (PW). Further, PW ionic concentrations of Fe, Ni (and possibly P) increased, as well as PW and soil pH that may led to higher stability of Ni-SOM complexes. A decrease was observed in labile Ni, perhaps due to excessive uptake and the increase in soil pH. A significant positive correlation between plant Ni and pseudo-total Ni was found although plant Ni concentrations did not follow as clearly a linear trend as pseudo-total soil Ni, whereas no significant correlations between plant Ni and labile Ni could be detected.*

4 Introduction

Several heavy metals and metalloids like Mn, Fe, Co, Cu, Ni, Zn, Mo are essential for regular plant metabolism and growth but become phytotoxic if certain concentration regimes are exceeded (Rascio and Navari-Izzo, 2011). Others like As, Se, Cd, Hg, Pb are not known to be important for any physiological function of plants making them undesirable for them in any way (Rascio and Navari-Izzo, 2011). Metal toxicity of both essential or non-essential elements causes serious stress in plants and can manifest in stunted growth, uneven nutrient balance or hamper metabolomic processes like photosynthesis or respiration (Clemens, 2006; Krämer, 2010). However, some plants have developed strategies to withstand exposure to high concentrations of heavy metals and even grow and reproduce normally under those conditions (Rascio and Navari-Izzo, 2011). That can be achieved by different strategies. One possibility is to exclude heavy metals in soil from root tissues and thus prevent high concentrations from being translocated to the more toxically sensitive aboveground area of the plant, the "excluder" strategy (Baker, 1981; Hall, 2002) (Figure 2). "Indicator" species show linear increasing metal concentrations in their biomass at increasing soil concentrations, so they reflect soil metal

concentration in their biomass. (Baker, 1981; Kazakou et al., 2008). Lastly, there are "hyperaccumulator" plants that contain particularly high metal concentrations, several times higher than soil concentrations (Rascio and Navari-Izzo, 2011). The remarkable fact that these plants thrive while they tolerate exceptionally high concentrations of phytotoxic metals in their tissues drove scientists for decades of diverse research fields to study them and was also the impetus for this thesis.

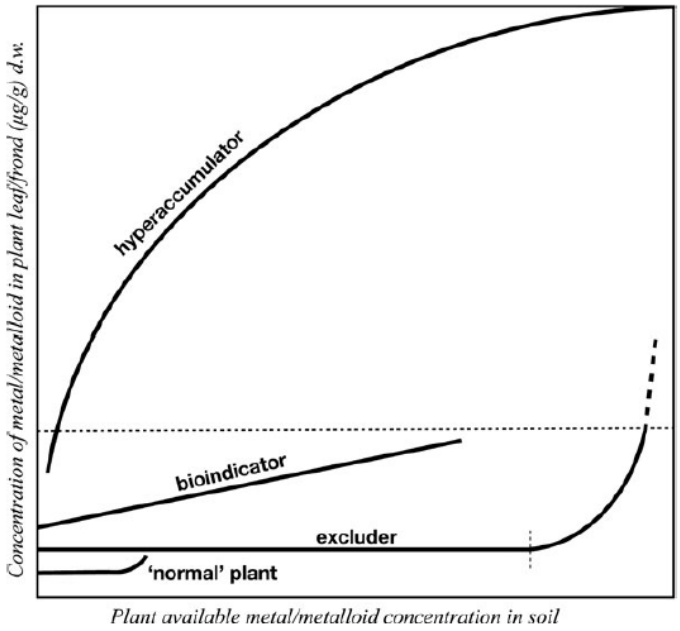

Figure 2: Conceptual diagram of metal uptake and avoidance strategies by plants after Baker (1981) from van der Ent et al. (2013).

4.1 Hyperaccumulator plants

Plants are classified as hyperaccumulators when they are able to take up large amounts of metals from soil and store them in their aboveground biomass without showing symptoms of toxicity (Baker and Brooks, 1989). Concentrations of trace elements vary greatly in soils and therefore there is a threshold value for each metal above which hyperaccumulation is defined (van der Ent et al., 2013). The threshold for Ni hyperaccumulation was first defined by Baker and Brooks (1989) and later revised by van der Ent et al. (2013) and is classified as Ni concentrations of 1000 µg g^{-1} dry weight in aboveground biomass. To date over 700 hyperaccumulator species have been discovered, accordingly around 0.2% of all vascular plants are described as hyperaccumulators making it quite a rare phenomenon (Reeves, 2003). However, the true number will likely be higher because this ability is still being described for new species. Counting more than 500 species most hyperaccumulator plants known today target at least Ni for accumulation (Reeves et al., 2018). This is presumably because Ni hyperaccumulation evolved as an adaptation to ultramafic outcrops that are high in Ni content and distributed worldwide (Cappa and Pilon-

Smits, 2014; Isnard et al., 2016). Those extreme sites often not only contain elevated concentrations of toxic elements but also a low supply of nutrients, like K, P and N and are characterised by an imbalanced Ca/Mg ratio making it arduous for the majority of plants to survive on them (Proctor and Woodell, 1975). Next to soils with a geogenic background of elevated metal concentrations there are anthropogenically contaminated sites which also can be colonised by hyperaccumulator plants and where they are found frequently (Cappa and Pilon-Smits, 2014).

The trait of hyperaccumulation has developed independently in distantly related plant families, with the *Brassicaceae* and the *Phyllanthaceae* having evolved the highest number of hyperaccumulator species (Reeves et al., 2021; Verbruggen et al., 2008). There are two regions where the majority of hyperaccumulator plants naturally occur: (i) the Mediterranean including Portugal, Italy, the Balkans, Turkey and adjacent countries and (ii) tropical and subtropical regions, especially New Caledonia, Cuba and some islands of Indonesia and the Philippines (Reeves et al., 2021).

Figure 3: Odontarrhena chalcidica, described as Alyssum murale in Waldstein-Wartenberg and Kitaibel (1799).

4.2 *Odontarrhena chalcidica*

Among all hyperaccumulator plants *Odontarrhena chalcidica* (Figure 3) is next to *Noccea goesingensis* and *Arabidopsis halleri* one of the most studied species because of its high potential for phytoremediation and phytomining (see chapter 4.3). It was first described by Waldstein-Wartenberg and Kitaibel (1799) under the name *Alyssum murale*. With the recent reestablishment of the genus *Odontarrhena* proposed by Španiel et al. (2015) it was renamed to *Odontarrhena chalcidica*. The plant belongs to the tribe of *Alysseae* in the family of *Brassicaceae* and is native to southeast Europe and the middle East with a rich representation in the Balkan peninsula (Al-Shehbaz, 1987; Dudley, 1964; Španiel et al., 2015). It is a perennial, evergreen plant with cauline,

subsessile leaves and is covered with short, fine whitish or greyish hairs (Dudley, 1964) (Figure 3). The stem usually grows 25 – 70 cm tall and is erect or ascending and can terminate in yellow panicle flowers (Flora of North America Association, 2010). It commonly grows upon ultramafic soils, on contaminated sites (e.g. waste heaps, former mining areas), next to roads or on barren and open field (Flora of North America Association, 2010).

4.3 Phytomining

The trait of hyperaccumulation was initially thought to bear great potential for remediation of contaminated sites by metal extraction of plants (phytoremediation) but over the years it proved to be neither cost-efficient nor rapid, at least for the element Ni (Chaney, 2018, 2021). Therefore, hyperaccumulation finds currently major application in the research field of phytomining whereby hyperaccumulator plants are harvested to obtain sufficient metals from the biomass to make it a profitable alternative to conventional mining (Chaney et al., 2021; van der Ent et al., 2015). Nickel is a promising candidate for phytomining since the majority of known hyperaccumulator plants target Ni, and many ultramafic areas (see chapters 4.4 - 4.6) and anthropogenically contaminated sites around the world offer opportunities to perform phytomining. Furthermore, the Ni price can make it currently economically profitable (Chaney et al., 2021; Reeves et al., 2018; van der Ent et al., 2015). In particular, recent price developments could give phytomining greater opportunities for the future, as LME (London Metal Exchange) cash price for Ni has increased by almost 30% from 2020 to 2021 attributed to high estimated demand for electric vehicle batteries and continued strong demand for stainless steel (U.S. Geological Survey, 2022).

Phytomining field experiments with *O. chalcidica/muralis (syn. Alyssum murale)* have already been conducted in the USA, Albania, Austria, Spain, and Greece (Li et al., 2003a; Bani et al., 2015a; 2015b; Kidd et al., 2018; Rosenkranz et al., 2019; Hipfinger et al., 2022; Pardo et al., 2018). *O. chalcidica* seems to be a promising phytomining candidate because it is a strong hypernickelophore, it grows erect which facilitates harvest has high biomass which increases yield and it is adapted to low-nutrient ultramafic soils which minimises fertilisation requirements (Chaney, 2018). In a five-year study Bani et al. (2015a) recorded an aboveground biomass of 9.00 t ha^{-1} of *O. chalcidica* per year with an average Ni concentration of 11.5 g kg^{-1} dry weight which results in a yield of 105 kg Ni ha^{-1} yr^{-1}. With a LME price of $ 21.6 kg^{-1} Ni (on August 10th 2022) this would result in a gross value of an annual phytomining crop of $ 2268 ha^{-1} yr^{-1} which could make it a highly profitable agricultural technology (Bani et al., 2015a). Especially in the Mediterranean region, where *O. chalcidica* is native, climatic conditions contribute to rapid biomass growth and the costs of land rent ($ 150 ha^{-1} yr^{-1}, Bani et al., 2015a) and production costs

($ 390 ha^{-1} yr^{-1}, Bani et al., 2015a) are quite low, so phytomining could have great potential in this region.

4.4 Serpentinites and ultramafic rocks

Serpentinites are ultramafic rocks mainly consisting of serpentine group minerals and subsequently soils derived from them are called serpentine soils (Proctor and Woodell, 1975). However, botanical and ecological literature often refers to soils as serpentine soils which, strictly speaking, were not formed mainly upon serpentinites but upon other ultramafic rocks such as peridotite (Alexander, 2004; Proctor and Woodell, 1975). Therefore, in this thesis, the term "ultramafic soil" is preferred to "serpentine soil", as it is more integrative with literature. Peridotites are ultramafic rocks that constitute > 90% of igneous ultramafic minerals, mainly pyroxene and olivine (Le Bas and Streckeisen, 1991). When these ultramafic rocks interact with aqueous fluids in settings like deep-sea hydrothermal vents, alkaline springs or the deep subsurface, they undergo a metamorphism called serpentinisation, by hydrating olivine and pyroxene to secondary serpentine minerals (Fritsch et al., 2021; Kelley et al., 2005; McCollom et al., 2016). Serpentine minerals that form during this process are 1:1 clay minerals following the ideal formulae $Mg_3Si_2O_5(OH)_4$ but variations in curvature of the layers, mostly by cationic substitution of Mg, lead to a high diversity of serpentine minerals (Echevarria, 2021; Fritsch et al., 2021). Mg commonly substitutes with other cations like Fe, Ni, Al, or Mn as a result of a lattice mismatch between the octahedral and tetrahedral sheets resulting in various crystalline structures with chemical impurities (Wicks and O'Hanley, 1988; Yariv and Heller-Kallai, 1975). There are three major serpentine mineral types to distinguish: The chrysotile (asbestos) form where curvature of the layers is most optimal and rolled (Yada, 1967), the lizardite form with more flat layers (Baronnet et al., 2007) and the antigorite form that is corrugated and wave-shaped (Fritsch et al., 2021; Mellini et al., 1987). Since serpentinisation is a process at the interface between hydrosphere and lithosphere, serpentinite rocks not only contain a high water content (up to ~13 wt% H_2O) but also many fluid-mobile elements like B, Li, As, Sb, Pb, U, Cs, Sr and Ba (Guillot and Hattori, 2013). Serpentinite are exceptionally high in Mg (18–24%) and high in Fe (6–9%) but contain low Ca (1–4%) and Al (1–2%) (Alexander, 2004). The colour of serpentinite rocks is greenish with an uneven pattern that comes from serpentine minerals occurring along with talc and other clay minerals that resembles snake skin and gives the name "serpentine" from Latin, "serpens", snake (Echevarria, 2021).

4.5 Ultramafic soils

Most of the soils developed on serpentine mineral containing rocks as parent material are classified as Cambisols or related soils and interestingly develop independent of latitude or elevation in a similar way worldwide (Echevarria, 2021; van der Ent et al., 2018). During pedogenesis serpentine minerals are generally unstable and degrade to secondary Fe-rich 2:1 phyllosilicates (e.g. smectite or low-charge vermiculite) that manifest as stable complexes in soil and limit further soil development (Bani et al., 2014; Bonifacio et al., 1997). The pH regime of serpentine soils ranges from alkaline soil pH towards neutral and slightly acidic but normally not substantially lower (e.g. Bonifacio et al., 1997; Chardot et al., 2007; Hseu et al., 2007; 2018; Kierczak et al., 2007). Due to the parent material, they show a very low Ca/Mg ratio and Mg generally dominates the cation exchange capacity (CEC) of serpentine soils (van der Ent et al., 2018). Mg as well as Si showed to leach down the soil profile owing to early weathering of serpentine minerals and as a consequence newly formed minerals are enriched in immobile Fe and in lower abundance Al in upper soil layers (Caillaud et al., 2004; 2006; 2009).

Another important characteristic of serpentine soils is their low fertility. On the one hand, this is due to the fact that the parent material and thus the soil on top of it contains little Ca and other important plant macronutrients P and K (Proctor and Woodell, 1975). On the other hand, high concentrations of heavy metals like Ni, Cr, Co but also Fe and Mn could induce toxicity to plants (Bani et al., 2014; Proctor and Woodell, 1975). Furthermore excess Mg that is present in serpentine soils could also bear stress to plants growing on them (Proctor and Woodell, 1975).

4.6 Nickel in serpentine soils

Soils around the world contain Ni in a very broad range, but mean concentrations of soil Ni are reported within the range of 13 – 37 mg kg^{-1} (Kabata-Pendias, 2011). However, Ni concentration is exceptionally high in serpentine soils with concentrations reported exceeding 10,000 mg kg^{-1} (Hseu et al., 2016; Oze et al., 2004). Reasons for that is their development from ultramafic rocks which are exceptionally high in Ni, Cr and Co content (Kabata-Pendias, 2011). Chemical weathering of these rocks produces accumulation of Ni and results in soils with high Ni concentrations, with levels commonly ranging above thousands of mg kg^{-1} (Gasparatos and Barbayiannis, 2019). However, the variability of Ni content in soils is spatially high and strongly influenced by geochemistry and mineralogy of the parent material as well as climate conditions, topography, biota and time (Caillaud et al., 2009; Gasparatos and Barbayiannis, 2019). Ni released from ultramafic rocks becomes mobile and is subsequently associated with secondary minerals which are mainly clay minerals (e.g. serpentines, chlorite or smectite) and Fe-/Mn

oxides (Massoura et al., 2006). In general, Fe-(oxy)hydroxides are assumed as important Ni hosts for surface horizons because they retain Ni when Si and other mobile elements like Mg or Ca are leaching down and accumulate in lower soil layers (Cheng et al., 2011; Gasparatos and Barbayiannis, 2019). In lower soil layers, clay minerals like talc, chlorite or smectite are mainly associated with Ni (Ratié et al., 2015). As pedogenesis progresses, Ni tends to be incorporated into crystal lattices of secondary minerals and thus is the majority of geogenic Ni found in mineral structures than complexed or surface charged to soil particles (Gasparatos and Barbayiannis, 2019; Kidd et al., 2009).

4.7 Nickel uptake and hyperaccumulation

Nickel is an essential micronutrient for plant growth because of its active site in the metalloenzyme urease, that catalyses urea to ammonia and bicarbonate (Dixon et al., 1975; Eskew et al., 1983; Polacco et al., 2013). Furthermore its role for other processes like glyoxylase or fungicidal benefits are debated (Dalton, 2018; Mustafiz et al., 2014). However, general plant demand for Ni is low and Ni scarcity is rare but still plants evolved a mechanism to regulate Ni homeostasis and subsequently Ni hyperaccumulation (Merlot et al., 2021). Ni follows the metal hyperaccumulation scheme of Figure 4 with stimulated metal uptake in roots, efficient xylem loading and transport followed by sequestration in leaves (Deng et al., 2018; Verbruggen et al., 2008).

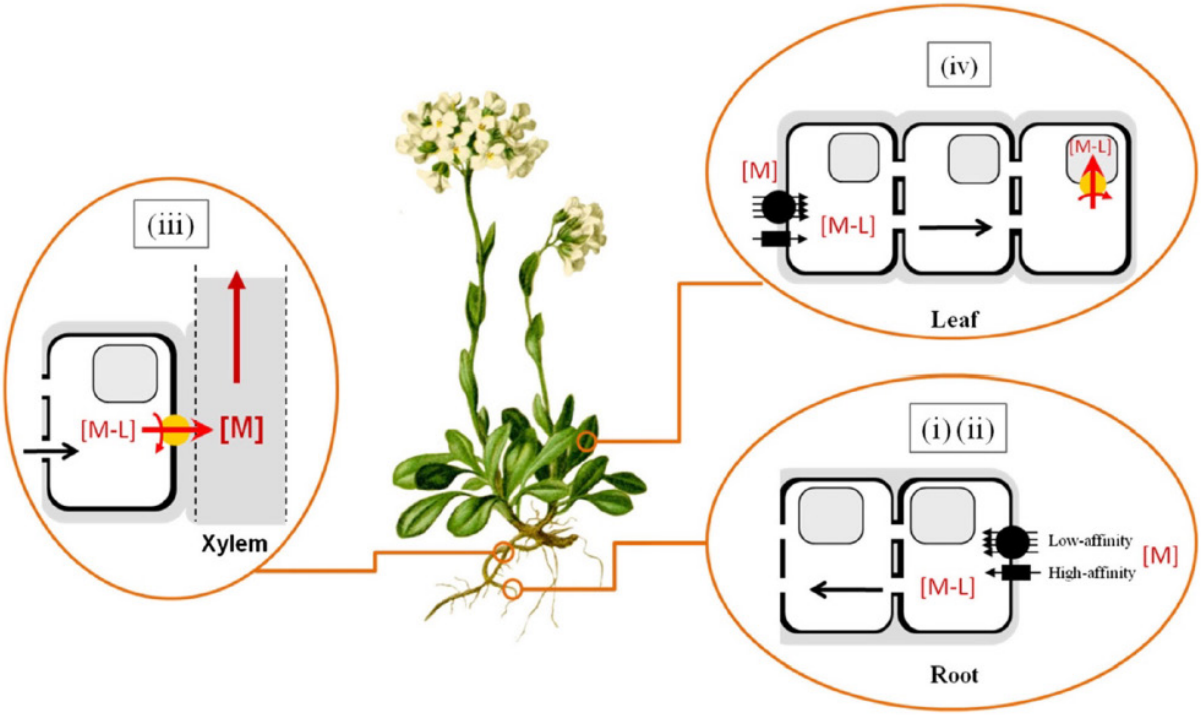

Figure 4: General mechanism of metal hyperaccumulation. [M] = metal cation, [L] = ligand, from Deng et al. (2018). Uptake of the metal mainly via low affinity cation transporters (i) and metal sequestration, i.e. detoxification by a ligand in root cells (ii) for higher metal tolerance in the plant. Afterwards effective xylem loading (iii) and root-to-shoot transport towards the leaves where the metal is sequestered and accumulated in leaf vacuoles (iv).

To date no specialised root cell Ni transporter has been characterised and several possibilities of plant Ni uptake are discussed that differ between plant genera or even species (van der Pas and Ingle, 2019). In general, it is suggested that Ni enters the root cell as free cation Ni^{2+} via poorly selective cation transporters (Figure 4, (i)) of the zinc transporter protein-(Zrt) or iron transporter protein-(Irt)like ZIP and IREG/Ferroportin families (Morrissey et al., 2009; Nishida et al., 2011; van der Pas and Ingle, 2019). Accordingly, Zn and Fe appear to be strongly linked to Ni uptake as all three elements mainly enter the root cell as divalent cations (Merlot et al., 2021). In line with that, Fe homeostasis interacts with Ni homeostasis in the non-hyperaccumulator *Arabidopsis thaliana,* suggesting that both metals share the same transporter (Nishida et al., 2011; Schaaf et al., 2006). In a recent study García de la Torre et al., 2020 elucidated the role of IREG/Ferroportins for Ni hyperaccumulation on a molecular level. They reported a threefold increase of Ni concentrations in roots of wild Ni hyperaccumulators under Fe deficiency compared to Fe repleted conditions supporting Ni uptake via Fe transporters (García de la Torre et al., 2020). Other experiments with species of the genus *Noccaea* showed that Ni was mainly taken up via Zn transporters. For hydroponic grown *Noccaea pindicum* and *Noccaea alpinum* var. *sylvium* equimolar concentrations of Zn/Ni lead to a reduction in leaf Ni content compared to a Ni only treatment (Taylor and Macnair, 2006).

In contrast, for two species of the genus *Odontarrhena* experiments showed very marginally to no effect of excess Zn concentrations on Ni hyperaccumulation (Mohseni et al., 2018). In fact, *O. bracteata* showed a strong increase in Ni uptake after one week of Fe starvation, suggesting that in this species Ni is taken up primarily via Fe-deficiency responsive Fe transporters (e.g. IRT 1 as suggested in Nishida et al., 2011) and that Ni and Fe compete for this transporter (Mohseni et al., 2018). However, in the same study the second species investigated, *Odontarrhena inflata,* was not significantly affected by Fe deficiency regarding Ni uptake (Mohseni et al., 2018). Interestingly, *O. bracteata* also showed reduced Ni hyperaccumulation when grown in a medium with increased Mn concentrations when root to shoot translocation remained constant, suggesting that Ni and Mn were competing at root cells (Ghaderian et al., 2015). Similar findings have been reported regarding Mn by Leigh Broadhurst et al., 2009 for *O. chalcidica*. Ni concentration in leaves decreased significantly when Mn concentration in the growing medium increased (from 0 to 40 mmol L^{-1}), which implies that Ni uptake of this species may also be impacted by phytoavailable Mn concentrations around the root (Leigh Broadhurst et al., 2009). Hence, Ni uptake kinetics of hyperaccumulators are complex and demand further understanding since they can be influenced by various cations (Mn^{2+}, Zn^{2+}, Fe^{2+}) and can differ between species of the same genus.

After taken up, chelation of Ni in the cytosol is suggested to play an important role in the metal tolerance mechanism of hyperaccumulator plants (van der Pas and Ingle, 2019) (Figure 4 (ii)). This is done in order to detoxify the metal and allows hyperaccumulator plants to take up high amounts of heavy metals and subsequently transport them into the leaves. In the case of several hyperaccumulators of the *Brassicaceae* family, root-to-shoot transport is considered to be mainly carried out by the amino acid histidine (His) (Ingle et al., 2005; Krämer et al., 1996). It is suggested that free His complexes Ni in root cells, is loaded into the xylem via specific transporters and translocates Ni to the shoot where it deposits in the shoot epidermis (Haydon and Cobbett, 2007; Kerkeb and Krämer, 2003; Küpper et al., 2001).

4.8 Nickel biogeochemistry in the rhizosphere

The term rhizosphere was first coined by Hiltner (1904) defining it as the soil zone influenced by plant roots and has later been refined by York et al. (2016) towards a dynamic view as integrating zones, processes and semantics influenced by roots that combines abiotic and biotic zones interactively to a holistic rhizosphere. That is done by passive and active release of root products like protons, hydroxyl ions, CO_2, and organic compounds and can substantially alter the physiochemical environment of the rhizosphere in terms of pH, redox potential or concentration of ligands (Hinsinger et al., 2005; Wenzel et al., 2018). Simultaneously, microbial communities also showed to be distinctly different in rhizosphere soil compared to bulk soil (Buée et al., 2009). Therefore, it is presumed that Ni biogeochemistry and mobility is modified by root activities.

In contrast to the general view that plants induce an acidification of the rhizosphere to mobilise metals and charge balance cation uptake with protons, several Ni hyperaccumulation studies rather observed an alkalinisation of the rhizosphere (Puschenreiter et al., 2003; Wenzel et al., 2004; Wenzel et al., 2018). Early findings of Wenzel et al. (2003) observed a slight increase in rhizosphere pH of *Noccaea goesingensis* grown on Austrian serpentine soil, suggesting that hydroxyl ions released during mineral dissolution were responsible for this. This was also observed in a recent study of Álvarez-López et al. (2021) when they found slightly elevated pH values in the rhizosphere of field grown hyperaccumulator *Odontarrhena serpyllifolia,* whereas an acidification in the rhizosphere of the excluder *Holcus lanatus* was observed. In line with that some studies found that Ni hyperaccumulation of *O. chalcidica* increased with increasing pH and decreased when soil pH was acidified (Kukier et al., 2004; Li et al., 2003b). As various factors influence the rhizosphere in complex interactions, several studies have attributed increased Ni mobility not to an enhanced pH solely, but rather to the result of various root-induced processes

occurring simultaneously (Kukier et al., 2004; Wenzel et al., 2004). However, more research is needed in this regard.

Nickel in the rhizosphere is furthermore exposed to rhizodeposition including plant mucilage, root lysates, and root exudates consisting of sugars, amino acids and a variety of low molecular weight compounds (Hirsch et al., 2013; Jones, 1998). Organic ligands from those compounds are able to complex free hydrated Ni^{2+} from soil solution and potentially enhance dissolution of Ni from minerals to maintain equilibrium solubility (Clemens et al., 2002; Wenzel et al., 2018). Therefore an important factor controlling plant available Ni is the pseudo-equilibrium between solid and aqueous soil phases (Kidd et al., 2009). Several studies observed a decrease in rhizosphere labile Ni due to plant uptake but an increase in Ni solubility presumably due to root-induced chelation of Ni (Puschenreiter et al., 2005; Wenzel et al., 2003). The increase in Ni solubility could as well be influenced by enhanced mineral dissolution of Ni-bearing phases induced by secretion of organic ligands as Chardot-Jacques et al. (2013) observed for the serpentine mineral chrysotile in the rhizosphere of Ni hyperaccumulator *Leptoplax emarginata*. They recorded a more than twofold increase in chrysotile dissolution in batches with *L. emarginata* compared to unplanted control (Chardot-Jacques et al., 2013). Interestingly, enhanced chrysotile dissolution was associated with a significant increase in pH which contributed to a release of hydroxyl ions during the mineral dissolution. This process could possibly also be linked to the rhizosphere alkalinisation mentioned above.

4.9 Aims of the work and research hypotheses

Although Ni hyperaccumulation has been investigated for over 40 years (Chaney et al., 2021), rhizosphere processes of Ni mobilisation remain poorly understood. Little is known about the role of root exudates in Ni mobilisation and the extent to which hyperaccumulator plants can influence the rhizosphere to take up Ni more efficiently. Various authors have addressed this question and reported different results depending on the methodology (e.g. Álvarez-López et al., 2021; Centofanti et al., 2012; Massoura et al., 2004; Puschenreiter et al., 2005; Wenzel et al., 2003). However, evidence is accumulating that hyperaccumulator plants actively mobilise Ni in the root zone. This question will therefore be further investigated, especially with regard to the relationship between Ni concentrations in soil and Ni accumulation in the plant. Especially, soil parameters such as pH or the concentration of organic ligands are likely to play an important role in this regard and can possibly be altered by root-mediated processes. Concurrently Ni, P and Fe biogeochemistry in soils and at the soil-plant interface are tightly linked and interactions of those elements are further elucidated. Iron is considered as important element during Ni hyperaccumulation because Ni in top soils is mainly associated with Fe oxides and probably

enters the plant cell via poorly selective Fe-transporters (García de la Torre et al., 2020; Gasparatos and Barbayiannis, 2019). Iron oxides in soils are also the mineral phase with which P is most associated, the nutrient that is highly deficient in serpentine soils and whose mobilisation is of great importance for hyperaccumulator plants (Bonifacio and Barberis, 1999). It is therefore important to look at these three elements at the same time and how they affect Ni hyperaccumulation, in particular the following research questions were tested:

Q 1 Are there indications for root exudation by the Ni hyperaccumulator *O. chalcidica*?

Q 2 Do root-induced processes affect soil solution in terms of pH and solubilization of Ni, Fe, and P?

Q 3 Is there a non-linear relationship between Ni concentrations in soil and Ni shoot uptake in *O. chalcidica*?

Q 4 Are changes in Ni solubility associated with changes of Fe- or P availability in the rhizosphere of *O. chalcidica*?

Q 5 Do different assessments of Ni availability lead to accordant results?

This study aims to enable a better understanding of rhizosphere processes and the role of soil characteristics during Ni hyperaccumulation. Insights into these processes may help to improve phytomining and promote a plant-based alternative to recycle Ni from soils. A pot experiment with *O. chalcidica* was performed along a gradient of pseudo-total and labile Ni plus an additional soil with high pseudo-total and low labile Ni. Soil parameters were characterised and the associated level of Ni hyperaccumulation investigated. Concurrently, soil pore water was monitored during the experiment and examined for indications of root-induced processes. This was done by analysing pore water for dissolved organic carbon (DOC) content as an indicator for root exudates. Concentrations of Ni and Fe in pore water were assessed to investigate Ni and Fe solubilisation processes in the rhizosphere. Labile fractions of Ni and Fe were compared before and after the experiment, as well as between planted and unplanted pots. The same procedure was used for P, only here an extraction assessing P bioavailability was used.

5 Material and Methods

5.1 Soil sampling

Soils for the pot experiment were taken from a forest area in close vicinity of the Austrian town Pilgersdorf next to a quarry (Figure 5). Previous studies already worked with soil from this area

because it is a known serpentine area and natural habitat of the Ni hyperaccumulator *Noccaea goesingensis* (Puschenreiter et al., 2005; Wenzel et al., 2003). The predominant land-use of the area is forestry. Although the site is located next to a quarry, the high Ni content in soil is a geogenic result of its serpentinite parent material and not due to anthropogenic contamination. In a first soil screening 14 locations were sampled and pseudo-total element concentrations (by *aqua regia* digestion) as well as DTPA- and $Sr(NO_3)_2$-extractable Ni concentrations were determined. Subsequently, soil from two locations were chosen for the experiment to create a gradient in Ni concentrations. The lowest Ni concentrations along the sampling gradient was soil 1 and the highest soil 6 (Figure 5). Those two locations were resampled and total element concentrations were confirmed in the field by a mobile XRF (x-ray fluorescence) device (Bruker Titan 600). An additional soil (soil LS) was added to the experiment as it was known to have high total Ni concentrations. Litter cover was removed and soils were sampled from topsoil layer and directly passed through a 4 mm steel sieve. A major difference between soil 1 and 6 towards soil LS was that the latter was subsoil exposed to the surface by a landslide, whereas soil 1 and 6 were topsoil samples. Samples were stored in PVC tubs and thoroughly air-dried for several weeks until analysed for soil chemical characterisation and setup of the pot experiment.

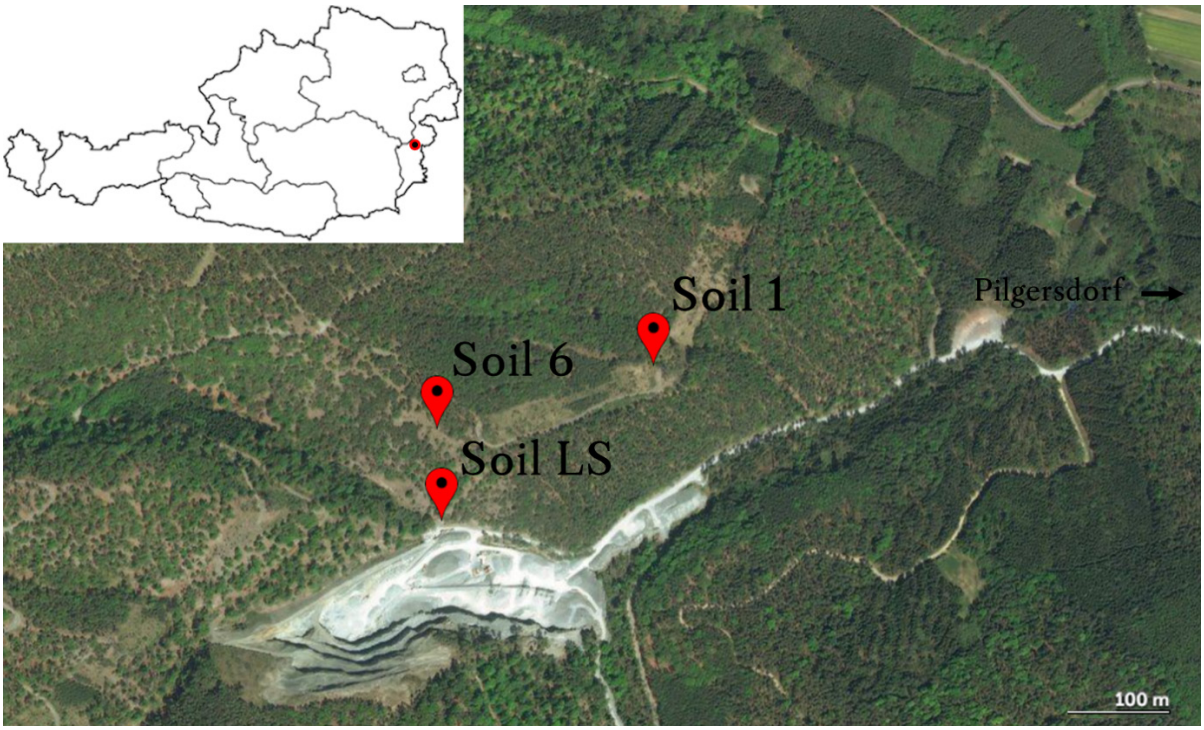

Figure 5: Study site including soil sampling locations next to the quarry mine and the location of the site within Austria

5.2 Pot experiment

A Ni gradient in labile and total element concentration was created by mixing soil 1 and soil 6 according to the soil mixing scheme (Table 1) obtaining a total of six experimental soils. Water content was determined (see 5.5.2) and soils mixed according to their dry weight.

Table 1: Soil mixing scheme

	Soil 1	**Soil 2**	**Soil 3**	**Soil 4**	**Soil 5**	**Soil 6**
% of Soil 1	100	80	60	40	20	0
% of Soil 6	0	20	40	60	80	100

450 g of each soil was weighed into PVC plant pots with fleece sheets in the bottom, to prevent particle loss, and a rhizon pore water sampler (Rhizosphere Research Products, Wageningen, NL) was inserted diagonally in each pot for pore water sampling (Figure 6). For the higher density of soil LS replicates the amount of soil was increased to 550 g in order to fully cover rhizon samplers with soil. Four experimental replicates were prepared for each soil, and an unplanted control without plants was included for each planted pot. Soils were left to equilibrate thoroughly for four weeks, applying cycles of wetting-drying to support soil equilibration and adhesion of soil to the rhizons. *Odontarrhena chalcidica* seeds were germinated in washed and air-dried vermiculite for seven days and then transplanted into the pot experiment. Starting point of the experiment was considered at transplantation time. Initially, four seedlings were added to each pot and 15 days after transplantation one plant was chosen to remain for the pot experiment. At this stage, the plants had three pairs of leaves. The decision on the plant candidate was based on comparable growth of the plants within the replicates. Plants were grown in a growth cabinet (CLF Plant Climatics, SE59-AR2cLED), with the following settings: 16 hours photoperiod from 5:30 pm to 9:30 am with a light intensity of 400 µmol photons m^{-2} s^{-1}, temperatures of 24 °C during the light period and 18 °C during the dark period, humidity maintained at 60%. The pots were arranged randomly and shuffled every two days, Soil moisture was kept gravimetrically at 60% water holding capacity (WHC) by daily watering (HQ water, conductivity: 0.055 < 0.080 mS) and was increased to 100% WHC before the pore water sampling (see chapter 5.3). No fertiliser was added during the whole experiment.

Figure 6: Rhizon sampler for pore water samplings in one of the pots for the experiment, own photography.

5.3 Pore water sampling

Soil solution was sampled four times according to Table 2 to examine pore water ionome, pH, dissolved organic carbon (DOC) and total bound nitrogen (TN_b). Sampling was conducted after 16 h light period since the day/night rhythm of the pot experiment was inverted. Pots were saturated to 80% WHC the day before sampling and at the sampling day gradually to 100% WHC and left to equilibrate for four hours. 10 ml of filtered (mean pore size of the rhizon samplers = 0.15 µm) pore water was sampled by connecting syringes to the rhizon samplers and divided into several aliquots for further analysis. Aliquots for DOC/TN_b and phosphorous measurements were stored latest 2 hours after sampling at -20 °C. Phosphorous content in solution was then determined colorimetrically after the molybdenum blue protocol of Murphy and Riley (1962) (see 5.5.8 for more details). To assess pore water DOC and TN_b, liquid total organic carbon (TOC) and bound nitrogen was measured after acidification of the samples with 10% HCl with an elemental analyser (Vario TOC Cube, Elementar). Aliquots for ICP-MS analyses were acidified to 2% HNO_3 with sub-boiled 65% HNO_3 and stored at room temperature (23 °C) until analysis. Pore water pH was determined immediately after sampling using a SCHOTT ProLab 4000 pH meter. The instrument was three-point calibrated at pH 4, 7, 10 and accuracy of the instrument was ensured by measuring calibration standard 7 every 10 samples.

Table 2: Timetable of the pot experiment. DAT = Days after transplantation of the plants into the pots.

DAT	0	7	21	49	71
	Plants transplanted	T_0	T_1	T_2	T_3

5.4 Plant analyses

5.4.1 Plant harvest and processing

Plant biomass was harvested 71 days after transplanting the seedlings into the pot experiment. Plant shoots were cut, thoroughly rinsed with deionised water, the fresh weight was noted, oven-dried at 60 °C for 38 hours and subsequently weighed again. Dried plant shoots were milled in scintillation vials by adding five ZrO_2 milling balls, shaken for three minutes at a frequency of 30 s^{-1} and subsequently stored until microwave assisted acid digestion.

Plant roots were carefully separated from soil by washing with deionised water, fresh weight noted, oven-dried together with the shoots and dry weight noted.

5.4.2 Shoot total element concentration

To investigate total elemental concentrations in plant biomass, a 150 mg oven-dried, milled subsample was weighed into Teflon microwave vessels. 3 ml 65% HNO_3 was added and left to react overnight. Then 0.76 ml 30% H_2O_2 was added and a microwave digestion of 25 minutes at 200 °C was performed in a CEM Mars 6 microwave oven. Digestions were diluted with 40 ml HQ water and analysed for macronutrients with ICP-OES (Optima 8300, PerkinElmer) and trace elements with ICP-MS (NexION 2000, PerkinElmer).

5.5 Soil analyses

A comprehensive characterisation of the initial soils was carried out to record the chemical composition of the soil in order to understand any influences during hyperaccumulation (Table 3). After the pot experiment soil samples were again analysed for DTPA, $Sr(NO_3)$ and Olsen-P extractions as well as soil pH to investigate possible changes due to the experiment (Table 3).

Table 3: Soil analytical overview. Analyses that were carried out on initial soils always contained three experimental replicates. The pot experiment contained four experimental replicates and an unplanted control for every planted pot.

Analysis	Initial soils	Soils after pot experiment
Aqua Regia	x	
DTPA extraction	x	x
$Sr(NO_3)_2$ extraction	x	x
$BaCl_2$ extraction (CEC)	x	
Olsen-P	x	x
pH	x	x

5.5.1 Water holding capacity (WHC)

To maintain soil moisture at an equal level the water holding capacity of the soils were determined. Therefore, four replicate pots of soils 1, 6 and LS were fully saturated with HQ water until leaching. Saturated pots were left to equilibrate for one hour and rewetted two more times. Saturated weight was taken and air-dried weight of the soils subtracted to get the water content held back in soil, formula (1). Water content for the soils 2 – 5 was calculated according to the soil mixing scheme Table 1.

$$WHC = \frac{mass\ soil\ wet\ [g] - mass\ soil\ dry\ [g]}{mass\ soil\ wet\ [g]} * percentage\ of\ saturation \quad (1)$$

5.5.2 Water content

Water content of the soils was determined to mix soils according to their dry mass and to correct soil extractions. Therefore 30 g soil was weighed in porcelain dishes and oven dried for 24 h at 105 °C. The exact weight of the sample was determined before and after drying and water content calculated after formula (1) where percentage of saturation holds 100%.

5.5.3 Soil pH

The pH of soil samples before and after the pot experiment was determined in ultra-pure H_2O with a w/v ratio of 1:2.5. For that, 25 mL of HQ water (conductivity: 0.055 < 0.080 mS) was added to 10 g of < 2 mm sieved, air-dried soil in 50 mL vials. Samples were thoroughly shaken by hand and then left to equilibrate for 2 hours. Then pH was determined in about 0.5 cm depth in solution with a SCHOTT ProLab 4000 pH meter. The instrument was three-point calibrated at pH 4, 7, 10 and accuracy of the instrument was ensured by measuring calibration standard 7 every 10 samples.

5.5.4 Soil pseudo-total element concentration

To assess pseudo-total element concentration of the soils, an *aqua regia* digestion was performed after ÖNorm L 1085 (2009). 0.5 g of air-dried and milled soil was weighed into microwave Teflon vessels. 4.5 mL of 37% HCl and 1.5 mL of 65% HNO_3 were added and the samples left in the fume hood to react overnight. On the next day digestion was performed at 200 °C for 40 min in a CEM Mars 6 microwave oven. After cooling down, Teflon vials samples were diluted with 50 ml HQ and the digest stored until analysis with ICP-MS (NexION 2000, Perkin Elmer) and ICP-OES (Optima 8300, PerkinElmer).

5.5.5 $Sr(NO_3)_2$ extraction

The $Sr(NO_3)_2$-extractable fraction of soils assesses free hydrated ions in solution that can be exchanged with the strontium salt of $Sr(NO_3)_2$ (Madden, 1988). This procedure appears to be a good estimation of readily available Ni for hyperaccumulator plant uptake (Everhart et al., 2006) and has the advantage of not altering soil pH or omitting chlorides that could possibly interfere with the substrate (Kukier and Chaney, 2001). An adapted method of Madden (1988) was performed by using 20 mL of 0.01 M $Sr(NO_3)_2$ solution to 5 g of soil that were shaken for 2 hours at 20 rpm in an overhead shaker. Afterwards, samples were filtered (Munktell Grade 1290, retention rate 3 – 5 µm) and acidified to 2% with sub-boiled 65% HNO_3 and stored at room temperature until dilution for analysis with ICP-MS (NexION 2000, PerkinElmer). Measured metal concentrations in $Sr(NO_3)_2$-extracts were corrected with the soil water content determined as explained in in section 5.5.2.

5.5.6 DTPA extraction

Isotopic exchangeable metal fractions of soils can be assessed by a single diethylene triamine pentaacetic acid (DTPA) extraction as developed by Lindsay and Norvell (1978) and refined for Ni by Echevarria et al. (2006). DTPA-extractable metal fractions were determined for both the initial and post-experimental soils. Extraction solution consisted of 0.005 M DTPA, 0.01 M $CaCl_2$ and 0.1 M TEA (triethanolamine) in HQ water, adjusted to pH 7.3 with 6 M HCl. For the extraction, 20 mL of DTPA solution was added to 10 g of soil sample and subsequently shaken for 2 hours at 20 rpm in an overhead shaker. Extractions were passed through folded paper filters (Munktell Grade 1290, retention rate 3 – 5 µm), acidified to 4.3% with sub-boiled 65% HNO_3 and stored at room temperature until further diluted for analysis with ICP-MS (NexION 2000, PerkinElmer). Water content was determined again as in section 5.5.2 to correct measured values according to the dry weight of the soils.

5.5.7 $BaCl_2$ extraction – Cation Exchange Capacity (CEC)

In order to analyse CEC and exchangeable macronutrients of the initial soil samples a $BaCl_2$ extraction was performed after ÖNorm L1086-89 (1989). Hereby the soils were exposed to a strong electrolyte ($BaCl_2$) and concentration of exchanged components determined and summed up. For that 2.5 g of < 2 mm sieved soil was weighed into shaking bottles, 50 mL of 0.1 M $BaCl_2$ solution added and subsequently gently shaken. Samples were left to react with the solution overnight, shaken at 20 rpm for 2 hours the next morning and then passed through folded paper filters (Munktell Grade 1290, retention rate 3 – 5 µm). The filtrate was acidified with sub-boiled 65% HNO_3 to 2% HNO_3 and diluted for analysis with ICP-OES (Optima 8300, Perkin Elmer). Measured concentrations of Ca, Mg and K were used to calculate the cation

exchange capacity of the soils. The amount of each substance was corrected for their water content and molar mass and then multiplied by their ionic charge to convert to $cmol_c\ kg^{-1}$. Concentrations of exchangeable cations were summed up to gain the cation exchange capacity.

5.5.8 Olsen-P

Plant available phosphorus content was assessed according to the protocol of Olsen (1954) as described by Schoenau and O'Halloran (2008) in Carter and Gregoric (2008). Accordingly, 2.25 g of sieved < 2 mm, air dried soil was weighed into 100 ml PE shaking bottles in triplicates. 45 ml of 0.5 mol L^{-1} $NaHCO_3$ (pH adjusted to 8.5 with 1 mol L^{-1} NaOH) was added, the samples shaken at 20 rpm for 30 minutes in an overhead shaker and subsequently passed through folded paper filters (Munktell Grade 1290, retention rate 3 – 5 µm). To remove remaining carbonate species from solution, 5 mL of Olsen-extract were diluted with 5 mL 0.25 mol L^{-1} H_2SO_4. Afterwards the diluted extracts were measured after the molybdenum blue protocol from Murphy and Riley (1962). Plant available P concentrations were determined with a UV/VIS spectrophotometer (Tecan infinite M nano$^+$). Values were as well corrected according to the water content of the soils.

5.6 Statistical Analyses

Differences in physiochemical parameters of pore water, plant and soil samples between planted replicates among all seven soils of the experiment were assessed using two-way ANOVA with Tukey's HSD post-hoc test. If normal distribution was not met data was either log-transformed or non-parametric Kruskal-Wallis H test was applied, followed by Wilcoxon rank sum test . Differences between planted and unplanted replicates within each soil group were assessed using Student's t-test. If normal distribution was not met, data were either log-transformed or a non-parametric Mann-Whitney-U test applied. To test for correlation between two variables Pearson's product-momentum correlation was performed after checking for normality and homoscedasticity of the data. All statistical analyses were carried out using R version 4.2.2 (2022-10-31) with the complementary R-Studio interface. Sample size was n = 4 for pore water, plant, and soil samples after the pot experiment and n = 3 for initial soil samples, a significance level of $p < 0.05$ was used.

6 Results

6.1 Initial soil characterisation

An overview of initial soil element concentrations and pH before the pot experiment is given in Table 4. *Aqua regia* digestion as well as DTPA- and $Sr(NO_3)_2$ extraction confirmed that mixing

of soils 1 and 6 successfully created a Ni gradient in both labile and pseudo-total concentration (Table 4). Pseudo-total Ni concentration ranged from 552 mg kg^{-1} in soil 1 to 1465 mg kg^{-1} in soil 6. DTPA-extractable Ni concentrations increased comparably from 41.6 mg kg^{-1} in soil 1 to 158 mg kg^{-1} in soil 6. Soil LS being subsoil showed the highest pseudo-total Ni concentration (1613 mg kg^{-1}) while the labile fraction of it is comparable with the low Ni soil 1 (53.1 mg kg^{-1}). Regarding nutrient concentrations, soil 1 was higher in pseudo-total K (2.23 g kg^{-1}) and Na (167 mg kg^{-1}) and concentrations decreased to 1.03 g kg^{-1} K and 21.4 mg kg^{-1} Na for soil 6 (Table 4). Phosphorous, S and Fe showed the opposite trend with lowest concentrations in soil 1 and highest in soil 6. Soil LS showed comparable concentration regimes regarding Fe, Mg, K and Na with soils 1 to 6 but was considerably higher in S (732 mg kg^{-1}) and lower in pseudo-total P (131 mg kg^{-1}).

Table 4: Characterisation of the experimental soils before the pot experiment. Pseudo-total element concentrations, DTPA- extractable metals, bioavailable Olsen-P, $Sr(NO_3)_2$-extractable metals and soil pH (in H_2O) of soils. Average values of n = 3 ± standard deviation. < LOQ = below limit of quantification.

	soil 1	soil 2	soil 3	soil 4	soil 5	soil 6	soil LS
	g kg $^{-1}$	g kg $^{-1}$	g kg $^{-1}$	g kg $^{-1}$	g kg $^{-1}$	g kg $^{-1}$	g kg $^{-1}$
Pseudo-total:							
Fe	56.3 ± 4.7	57.7 ± 3.9	60.1 ± 3.7	60.4 ± 6.3	66.5 ± 1.4	69.1 ± 1.8	59.3 ± 3.4
Mg	74.1 ± 5.7	87.4 ± 2.3	110 ± 16	117 ± 5.8	136 ± 4.4	151 ± 2.3	136 ± 4.1
Ca	4.18 ± 0.4	3.82 ± 0.4	3.79 ± 0.6	3.41 ± 0.5	2.33 ± 0.1	1.66 ± 0.2	5.36 ± 0.5
K	2.23 ± 0.1	2.28 ± 0.3	2.04 ± 0.4	1.95 ± 0.2	1.32 ± 0.04	1.03 ± 0.1	2.06 ± 0.6
	mg kg $^{-1}$	mg kg $^{-1}$	mg kg $^{-1}$	mg kg $^{-1}$	mg kg $^{-1}$	mg kg $^{-1}$	mg kg $^{-1}$
Ni	552 ± 52	715 ± 75	857 ± 60	1026 ± 74	1249 ± 46	1465 ± 58	1613 ± 8.3
Cr	1142 ± 129	1212 ± 125	1500 ± 302	1524 ± 102	1981 ± 248	2040 ± 100	1326 ± 93
Mn	1079 ± 31	1083 ± 60	1119 ± 42	1148 ± 12.1	1304 ± 61	1334 ± 39	1104 ± 55
Co	72.4 ± 1.8	75.9 ± 3.8	80.8 ± 0.8	88.4 ± 5.0	106 ± 13	113 ± 4.1	107 ± 2.9
Cu	13.1 ± 1.5	16.7 ± 3.9	14.9 ± 0.4	18.1 ± 2.1	19.2 ± 0.9	21.7 ± 2.4	40.6 ± 2.4
Zn	62.7 ± 1.5	63.4 ± 8.6	65.0 ± 5.3	60.3 ± 0.9	70.6 ± 8.3	59.4 ± 1.4	53.4 ± 5.5
P	235 ± 14	252 ± 9.9	257 ± 35	259 ± 12	281 ± 10	297 ± 20	131 ± 6.8
S	334 ± 3.5	370 ± 35	369 ± 58	390 ± 11	372 ± 19	414 ± 34	732 ± 53
Na	167 ± 16	166 ± 30	163 ± 47	125 ± 31	51.8 ± 5.2	21.4 ± 11	64.5 ± 47
DTPA							
Ni	41.6 ± 0.5	61.8 ± 0.7	84.9 ± 2.4	107 ± 1.4	137 ± 7.2	158 ± 7.1	53.1 ± 0.6
Fe	317 ± 1.9	300 ± 2.8	275 ± 4.0	255 ± 1.3	250 ± 5.9	212 ± 7.9	17.5 ± 0.7
Cr	< LOQ	< LOQ	< LOQ	< LOQ	< LOQ	< LOQ	< LOQ
Co	3.20 ± 0.05	2.19 ± 0.2	2.75 ± 0.1	1.91 ± 0.03	1.88 ± 0.02	1.78 ± 0.1	0.57 ± 0.04
Cu	0.87 ± 0.1	1.09 ± 0.2	1.23 ± 0.03	1.52 ± 0.02	2.70 ± 1.3	2.08 ± 0.1	1.61 ± 0.02
Zn	4.02 ± 0.2	3.48 ± 0.4	3.07 ± 0.1	2.77 ± 0.1	2.69 ± 0.1	2.21 ± 0.3	0.30 ± 0.1
Olsen-P	2.94 ± 0.1	3.53 ± 0.4	3.59 ± 0.2	4.21 ± 0.5	6.20 ± 0.2	6.51 ± 0.9	1.17 ± 0.2
	µg kg $^{-1}$	µg kg $^{-1}$	µg kg $^{-1}$	µg kg $^{-1}$	µg kg $^{-1}$	µg kg $^{-1}$	µg kg $^{-1}$
$Sr(NO_3)_2$							
Ni	641 ± 1.8	809 ± 15	920 ± 10	1033 ± 14	1157 ± 19	1247 ± 9.0	376 ± 14
Fe	52.4 ± 4.7	56.8 ± 9.2	77.4 ± 20	63.3 ± 32	108 ± 94	117 ± 104	43.8 ± 28
Cr	10.8 ± 0.7	10.2 ± 0.4	13.6 ± 5.0	11.5 ± 2.5	12.3 ± 0.4	< LOQ	< LOQ
Co	84.7 ± 2.7	40.8 ± 3.1	36.8 ± 0.5	18.6 ± 0.2	17.3 ± 0.9	12.7 ± 0.5	4.31 ± 0.2
Cu	17.0 ± 6.5	10.6 ± 3.3	9.84 ± 2.5	68.5 ± 95	15.8 ± 3.4	8.36 ± 17	4.45 ± 0.6
Zn	135 ± 1.3	103 ± 1.2	87 ± 7.6	106 ± 66	61 ± 5.7	210 ± 1.4	33.8 ± 0.8
	$cmol_c$ kg^{-1}	$cmol_c$ kg^{-1}	$cmol_c$ kg^{-1}	$cmol_c$ kg^{-1}	$cmol_c$ kg^{-1}	$cmol_c$ kg^{-1}	$cmol_c$ kg^{-1}
CEC	18.8 ± 0.2	20.0 ± 0.6	21.4 ± 0.5	22.5 ± 0.4	24.3 ± 1.3	27.5 ± 0.8	14.1 ± 0.1
	[-]	[-]	[-]	[-]	[-]	[-]	[-]
pH	5.93 ± 0.03	6.11 ± 0.06	6.18 ± 0.01	6.25 ± 0.02	6.33 ± 0.01	6.48 ± 0.08	8.08 ± 0.03

According to the soil mixing scheme (Table 1) pseudo-total trace element concentrations of Cr, Mn, Co, Cu increased gradually, whereas the labile fractions of Co and Cu rather showed a decreasing trend from soil 1 to soil 6. All soils of the experiment show very low concentrations of plant-available P. The lowest Olsen-P values were found in soil LS (1.17 mg kg^{-1}), marginally higher in soil 1 (2.94 mg kg^{-1}) and highest in soil 6 (6.51 mg kg^{-1}). CEC increased from 18.8 $cmol_c$ kg^{-1} in soil 1 to 27.5 $cmol_c$ kg^{-1} in soil 6. Soil LS showed the lowest CEC with 14.1 $cmol_c$ kg^{-1}. Soil pH ranged from slightly acidic in soil 1 (5.93) towards nearly neutral (6.46) in soil 6 and was alkaline in soil LS (8.08).

6.2 Plant biomass

Figure 7: Growth stage of O. chalcidica 71 days after transplanting seedlings into the pot experiment.

Mean values of plant dry weight (DW) divided into shoots and roots are presented in Table 5 (Supplementary Material, p. 60) and Figure 8. Lowest in biomass were replicates from soil 1 (477 mg DW) and highest from soil 6 (946 mg DW). Shoot biomass was significantly higher for plants grown in soil 6 compared to soil 1 to 5 but in the same range than plants from soil LS (Figure 7, Figure 8 a). Soils 1 to 5 did not show any differences in dry weight of the shoots, and only plants of soil 1 had a significantly lower biomass than those of soil LS. Values for root biomass ranged from 297 mg DW (soil 2) to 385 mg DW (soil 6) resulting in substantially lower and less spread root than shoot biomass (Table 5). Mean root DW showed no significant differences across the whole experiment (Figure 8 b).

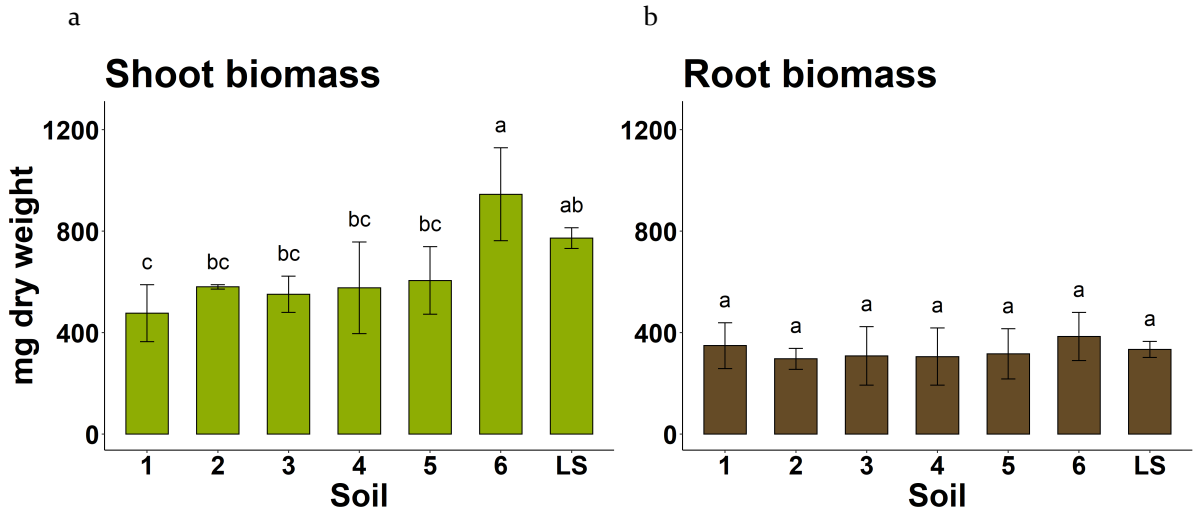

Figure 8: Shoot (a) and root (b) dry weight of O. chalcidica 71 days after transplanting seedlings into the pot experiment. Average values (n = 4) ± standard deviation, letters indicate significance between pots (p < 0.05).

Mean concentrations of elements measured in microwave digested shoots of *O. chalcidica* are also presented in Table 5 (Supplementary Material, p. 60) and Figure 9. Fe concentrations ranged from 41 to 62 mg kg^{-1} and did not show any significant differences between the soils. Plant P concentrations were about 100 times higher and ranged from 552 to 900 mg kg^{-1}. Plants grown on soils 1 to 5 did not show significant differences in P concentration (Figure 9 b). However, plants grown on soil LS and soil 6 contained significantly elevated P concentrations in shoots compared to plants from soil 1 to 5 (Figure 9 b). Ni in shoots of *O. chalcidica* did not entirely follow the linear pattern according to the soil mixing scheme (Table 1) but followed the trend of lowest Ni concentrations in plants of soil 1 and 2 (2442 and 3873 mg kg^{-1}) and highest Ni concentrations in plants of soil 6 and LS (7667 and 7514 mg kg^{-1}, Figure 9 c). However, soil 4 and 5 showed plant Ni concentrations in the same range as soils 1 to 3 without significant differences. Normalised to the dry weight of each plant a Ni yield per plant was calculated and showed highest Ni extraction in soil 6 (7277 µg $plant^{-1}$) followed by soil LS (5808 µg $plant^{-1}$) and was lowest in soil 1 (1125 µg $plant^{-1}$) (Table 5, Supplementary Material).

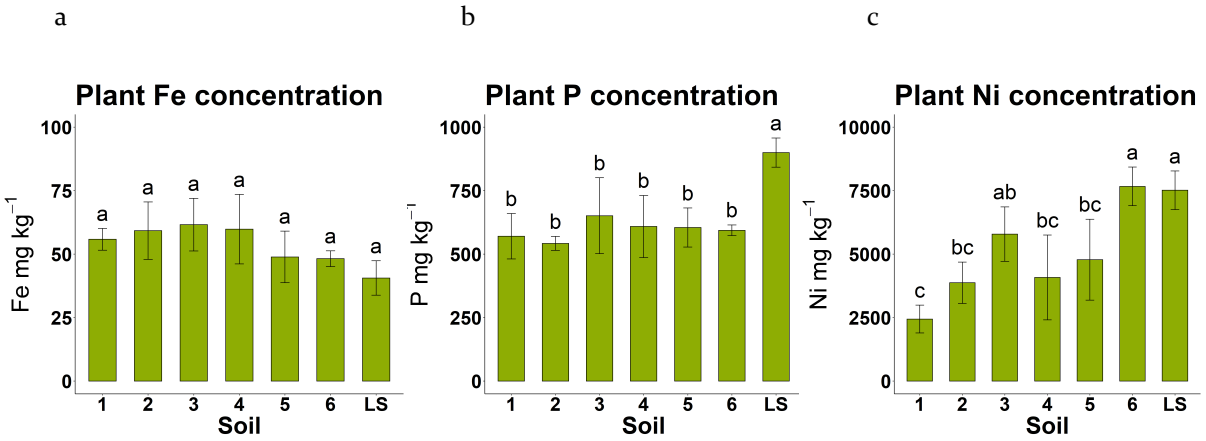

Figure 9: Elemental concentrations of Fe (a), P (b) and Ni (c) in shoots of O. chalcidica. Scale of y-axis increases 100fold per plot respectively. Average values (n = 4) ± standard deviation, letters indicate significance between soils (p < 0.05).

6.3 Changes in soil characteristics after the pot experiment

To investigate changes in soil chemical characteristics by the pot experiment, planted and unplanted control pots were analysed for labile fractions (DTPA- and $Sr(NO_3)_2$-extractable) of trace metals as well as bioavailable Olsen-P and soil pH. Results of DTPA- and $Sr(NO_3)_2$-extractable are listed in Table 6 (Supplementary materials) and in Figure 5.

Both labile fractions showed higher values for Ni in control pots after the experiment compared to the initial characterisation (Table 4, Table 6 Supplementary Material p. 61). Regarding the DTPA extraction Ni concentrations increased at least by 6 (soil 1) to 30 (soil 6) mg kg^{-1} Ni, which accounted for a difference of 14 – 19% respectively. $Sr(NO_3)_2$-extractable Ni increased by 194 µg kg^{-1} in soil 1 (30%) up to 458 (soil 3) µg kg^{-1} (54%). Only soil LS showed $Sr(NO_3)_2$-extractable Ni values 820 µg kg^{-1} lower in controls after the pot experiment compared to initial soils. DTPA-extractable Ni in control pots was around 100 times higher than the $Sr(NO_3)_2$-extractable fraction of soils after the pot experiment (Figure 10). Both labile fractions showed significantly lower Ni concentrations in planted pots compared to unplanted controls nearly across all soils. This significance was more pronounced for the $Sr(NO_3)_2$-extractable Ni fraction than for DTPA-extractable (Figure 10 b).

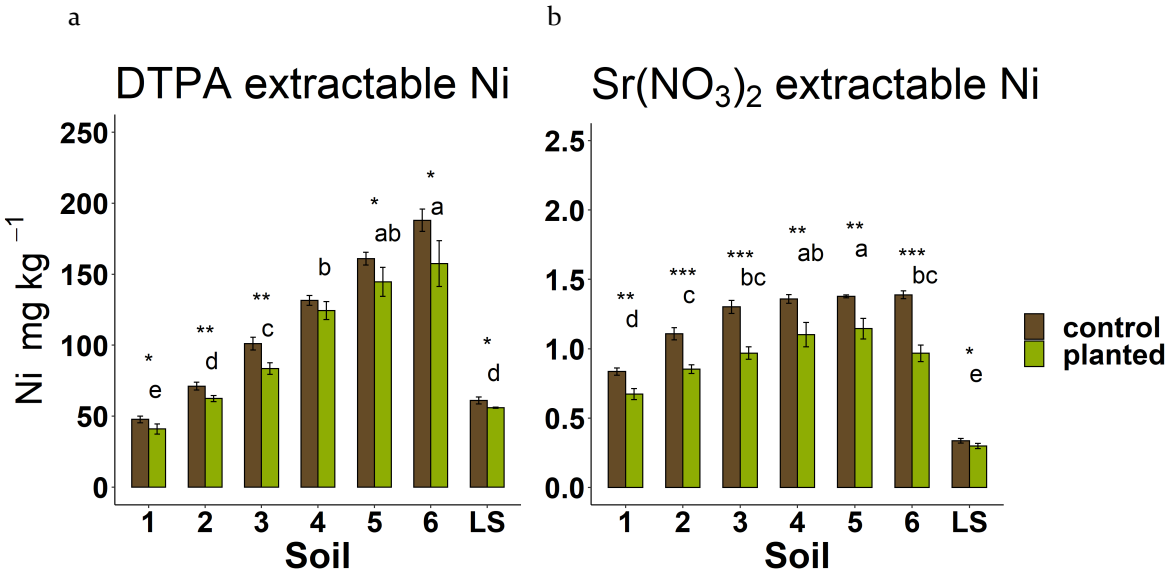

Figure 10: Labile Ni fractions in mg kg^{-1} of soils after the pot experiment for planted (green) and unplanted (brown) pots. Note the 100-fold decreased y-axis for $Sr(NO_3)_2$-extractable Ni (b). Average values (n = 4) ± standard deviation, asterisks: p < 0.05 "", p < 0.01 "**", p < 0.001 "***" indicate significance between planted and control pots, letters indicate significance (p < 0.05) between planted pots*

After the pot experiment soil pH still followed the pattern of the soil mixing scheme (Table 1) with a gradual increase from soil 1 to 6 for both planted and unplanted pots. However, pH values of control pots across the whole experiment decreased by values of 0.24 to 0.34 for soils 1 to 6 and by 0.09 for soil LS compared to the initial soils, For planted pots of soils 1 to 6 a significant alkalinisation of the soils by averaged values of 0.19 – 0.34 compared to control pots occurred (Figure 11). Contrastingly, for soil LS no significant changes in soil pH were measured.

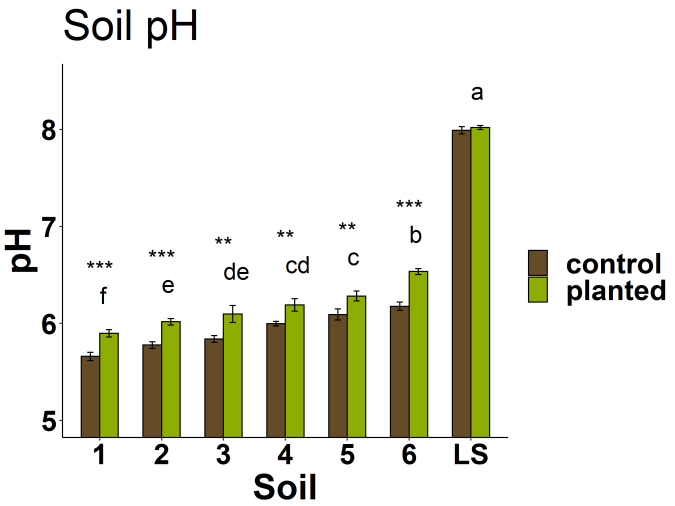

Figure 11: Soil pH of planted (green) and unplanted (brown) pots after the pot experiment. Average values (n = 4) ± standard deviation, asterisks p < 0.05 "", p < 0.01 "**", p < 0.001 "***" indicate significance between planted and control pots, letters indicate significance (p < 0.05) between planted pots.*

Plant available P (Olsen-P) did not show any significant changes between both planted and unplanted soils and within soils 1 to 6 (Figure 12). Values for those soils ranged from 5 to 10 mg kg^{-1} P and were thus significantly higher than soil LS, where generally lower values for P were measured, but the control pots had significantly higher concentrations compared to the planted replicates (Figure 12).

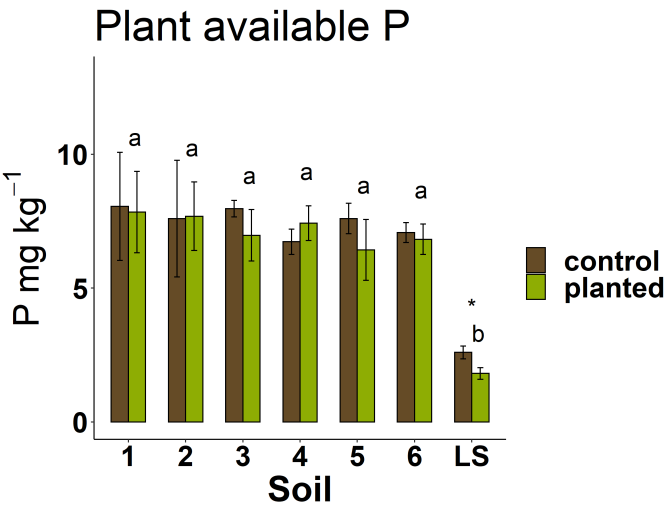

Figure 12: Plant available P, after Olsen (1954), of planted and unplanted soils after the pot experiment. Average values (n = 4) ± standard deviation, asterisks: p < 0.05 "", p < 0.01 "**", p < 0.001 "***" indicate significance between planted and control pots, letters indicate significance (p < 0.05) between planted pots.*

6.4 Pore water

Results of pore water samples are displayed in Figure 13 - Figure 15 with one plot per sampling time T_0 – T_3 from the start of the experiment 7 days after transplantation of seedlings into the pot experiment until the harvest 71 days after transplantation.

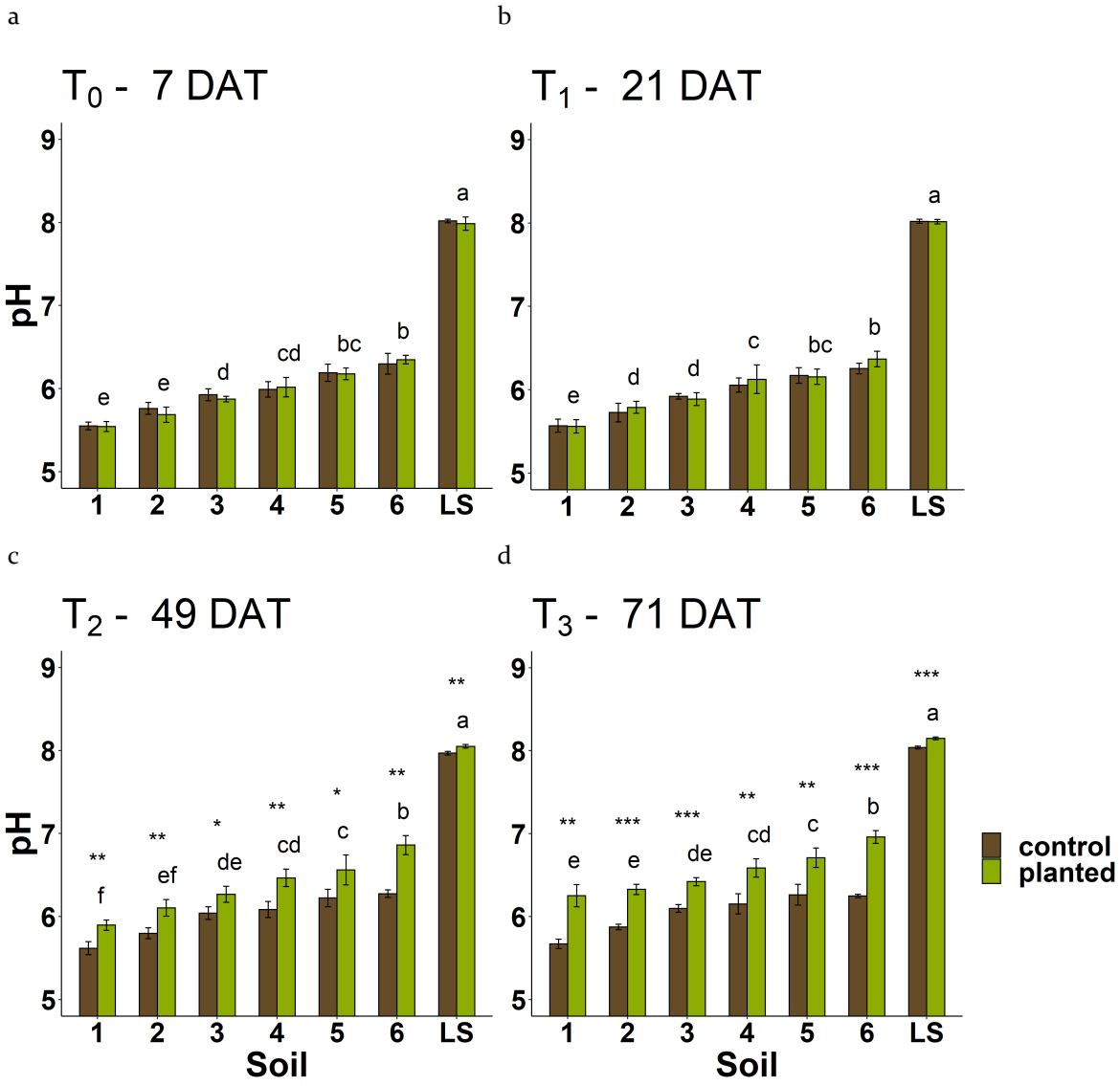

Figure 13: pH of pore water samplings T_0 (a) - T_3 (d) of planted (green) and unplanted (brown) pots Average values (n = 4) ± standard deviation, asterisks: p < 0.05 "", p < 0.01 "**", p < 0.001 "***" indicate significance between planted and control pots, letters indicate significance (p < 0.05) between planted pots. DAT = days after transplantation of seedlings into the pot experiment.*

The pH of pore water from control pots are in line with values from the pH soil extraction and follow the soil mixing scheme. From T_0 to T_3 a slight increase in pH of controls, highest in soil 3 (0.17) and lowest in soil LS (0.02), occurred (Figure 13 a - d). Between planted and control pots no significant changes were measured for T_0 and T_1. However, for T_2 a significant increase in pH was noted for planted pots compared to control pots that further pronounced for sampling T_3. Alkalinisation of pore water pH in planted pots compared to controls ranged from 0.32 – 0.71 for soils 1 – 6 and was lower for soil LS (0.11) but still strongly significant.

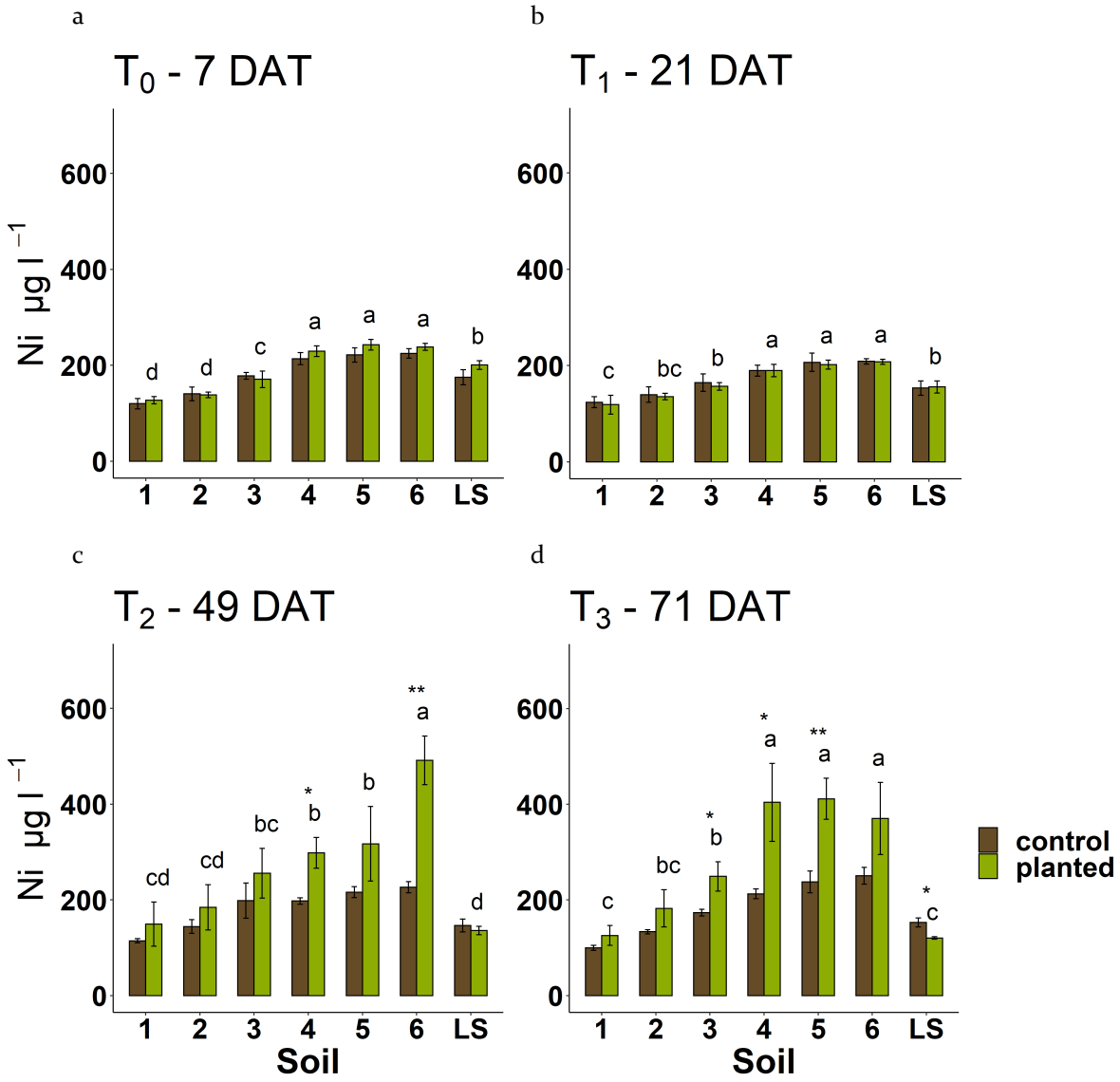

Figure 14: Ni concentrations of pore water samplings T_0 (a) - T_3 (d) of planted (green) and unplanted (brown) pots. Average values (n = 4) ± standard deviation, asterisks: p < 0.05 "", p < 0.01 "**", p < 0.001 "***" indicate significance between planted and control pots, letters indicate significance (p < 0.05) between planted pots. DAT = days after transplantation of seedlings into the pot experiment.*

For sampling time T_0 and T_1 no differences between planted and control pots were found while T_2 showed a significant increase of Ni in pore water of 100 and 265 µg l^{-1} on average for high Ni soils 4 and 6 (Figure 14 a -c). These differences account for an increase of 50% for soil 4 and 117% for soil 6. At T_3, no significant increase could be detected for soil 6 due to the high standard deviations of the samples, but soils 3, 4 and 5 showed significantly elevated Ni concentrations of 76 (44%), 191 (90%) and 174 (73%) µg l^{-1}, respectively (Figure 14 d). Interestingly, planted replicates of soil LS showed significantly lower Ni concentrations (-33 µg l^{-1}, 22%) in pore water than controls at T_3.

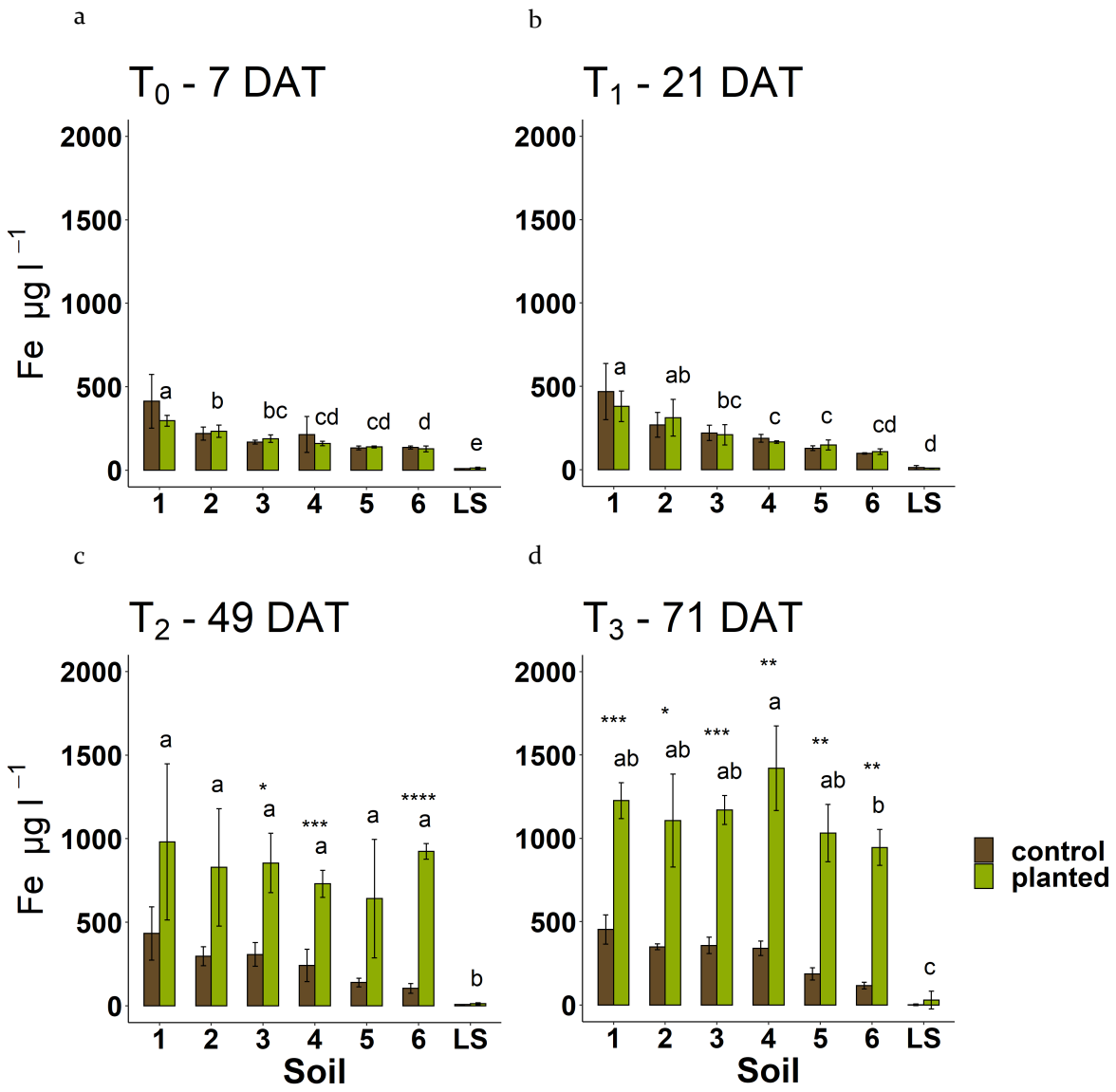

Figure 15: Fe concentrations of pore water samplings T0 - T3 of planted (green) and unplanted (brown) pots. Average values (n = 4) ± standard deviation, asterisks: p < 0.05 "", p < 0.01 "**", p < 0.001 "***", p < 0.0001 "****" indicate significance between planted and control pots, letters indicate significance (p < 0.05) between planted pots. DAT = days after transplantation of seedlings into the pot experiment. Samples of control soil LS were below limit of quantification (< 1.13 µg l-1).*

Dissolved Fe concentration in pore water remained unchanged between T_0 and T_1 followed by a strong increase at T_2 for most planted pots (Figure 15 a -c). This increase was significant for soil 3 and strongly significant for soils 4, and 6, whereas soils 1, 2 and 5 showed a large spread in the data. The increase for dissolved Fe in pore water was then also significant for soils 1 and 2 at T_3 when mean concentrations increased at least by 270% for soil 1 and up to 800% for soil 6 in planted pots compared to controls (Figure 15 d).

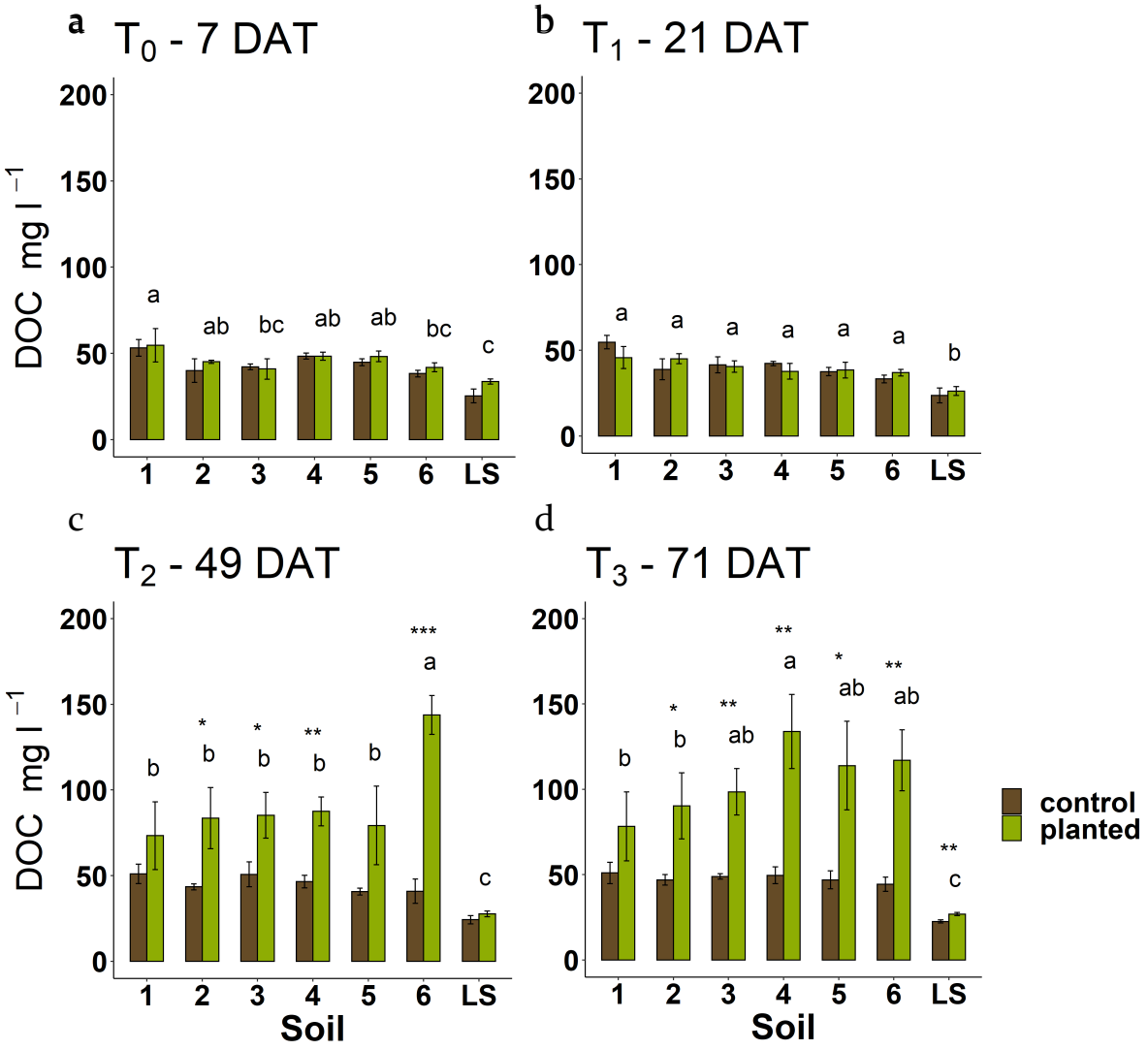

Figure 16: DOC concentrations of pore water samplings T0 to T3 of planted (green) and unplanted (brown) pots. Average values (n = 4) ± standard deviation, asterisks: p < 0.05 "", p < 0.01 "**", p < 0.001 "***", p < 0.0001 "****" indicate significance between planted and control pots of the same soil, letters indicate significance between planted pots. DAT = days after transplantation of seedlings into the pot experiment.*

DOC was determined in pore water for T_0 to T_3 (Figure 16). At T_0 and T_1 no significant differences between planted and unplanted pots were measured and values for all pots of the experiment were in a similar range between 30 and 50 mg l^{-1}. Control pots did not change DOC concentrations significantly for T_2 and T_3 as well. However, after 49 days at T_2 a strong increase in DOC of planted pots was recorded. This increase was significant for all soils 2, 3, 4 and 6 and was highest for soil 6. For T_3 soil 5 and LS as well increased significantly and soil 4 showed highest mean DOC concentrations (Figure 16).

Furthermore total N in pore water (TNb) was assessed throughout the pot experiment (Figure 18 Supplementary Material). No significant changes occurred for T_0 and T_1 but for T_2 a strong depletion of dissolved N in planted pots was recorded. This was significant for soils 5, 6 and LS whereas soils 1 to 4 showed lower mean values but no statistical significance. At T_3 TNb was

further reduced so that nearly all planted pots showed substantially low values. Control pots were reduced in TNb as well with the significantly highest values in soil 5 and 6 and the lowest in soils 1 to 3 (Figure 18 Supplementary Material).

Phosphorous in pore water could not be reliably determined due to the quantification limit of the method (20 µg l^{-1}). For the majority of the samples, P concentrations were at or below the quantification limit, resulting in very high standard deviations, so that it was not possible to make a clear statement about P content in pore water or to describe possible plant-induced changes.

7 Discussion

7.1 Experimental soil analysis

Pseudo-total element concentration analysis of all experimental soils (Table 4) confirmed Ni concentration regimes that are typical for ultramafic soils (Gonnelli and Renella, 2013; Hseu et al., 2018). Regarding the labile fraction, values for the labile Ni pool ranged from 41.6 mg kg^{-1} (soil 1) to 158 mg kg^{-1} (soil 6) in DTPA-extractable Ni and are well comparable with other studies (Bani et al., 2014; Bani et al., 2015a; Tognacchini et al., 2020). Therefore, the DTPA-extractable Ni fraction accounted for 3 to 11% of the pseudo-total concentrations (Table 4). $Sr(NO_3)_2$-extractable Ni ranging from 376 µg kg^{-1} (soil LS) to 1247 µg kg^{-1} (soil 6) compared also well to previous work on Austrian ultramafic soils like 532 µg kg^{-1} in Rosenkranz et al. (2019) but there are also other studies like Álvarez-López et al. (2021) who reported higher values (up to 12.5 mg kg^{-1}).

Other typical ultramafic soil properties such as the very high Mg/Ca ratio and deficiency in plant nutrients N and K were also observed for all soils (Table 4). Olsen-P extraction showed low values of plant-available P ranging from 1.17 to 6.51 mg kg^{-1}. This would indicate P deficiency if compared to the mean critical Olsen-P-extractable value of 19 mg kg^{-1} P for crops grown on European soils (at 95% confidence interval of the yield) (Nawara et al., 2017). Phosphorous critical values however can vary for different plant species (Nawara et al., 2017) and *O. chalcidica* is well adapted to nutrient deficient soils (Proctor and Woodell, 1975). Furthermore, element concentrations of Cr, Co, Fe, Mg and Ca are in ranges to be expected for ultramafic soils (Table 4). The range of 56.3 g kg^{-1} to 69.1 g kg^{-1} of pseudo-total Fe in soils of the present study is in good agreement with other work on ultramafic soils like 64 g kg^{-1} in Tognacchini et al. (2020). However, DTPA-extractable Fe of the soils 1 (317 mg kg^{-1}) to 6 (212 mg kg^{-1}, Table 4) is considerably higher than other studies that worked with European ultramafic soils like in Tognacchini et al. (2020) with 32.4 mg kg^{-1}, Bani et al. (2015a) 60 mg kg^{-1} or Hipfinger et al.

(2022) who reported 75.5 mg kg^{-1}. Soil LS as the soil type with general lower labile fractions is with 17.5 mg kg^{-1} DTPA-extractable Fe lower than soil 1 to 6 and the above-mentioned studies.

Along with Ni, large amounts of Cr are typically released by weathering of ultramafic rocks (Cheng et al., 2011; Oze et al., 2004) and highly elevated pseudo-total Cr concentrations were detected in the soils of this experiment. However, the large majority of Cr is immobile in aerobic soils, which explains why the labile fraction (DTPA-extractable) was very low and in most cases below the detection limit. The pH values of slightly acidic to alkaline are in well agreement with previous characterisations of ultramafic soils in literature (Bonifacio et al., 1997; Chardot et al., 2007; Hseu et al., 2007; 2018; Kierczak et al., 2007; Wenzel et al., 2003). The higher pH values of soil LS are probably due to the fact that the sample, as subsoil, was less exposed to weathering and less advanced in pedogenesis and soil acidification.

7.2 Plant growth and analysis

Odontarrhena chalcidica plants grew without signs of toxicity until the eighth week of the experiment, when plants on all soils began to show signs of yellowish to reddish-purple discolouration of the older leaves and the experiment was terminated after 71 days to avoid interference with the experiment by leaf fall. The reason for the symptoms could not be clearly determined, a nutrient deficiency of P would be possible, as the nutrient showed critically low values in the shoot biomass, but it could also be related to watering (suffering from water soil saturation before pore water sampling) or a mixture of insufficiencies.

Plant biomass has not been influenced by the Ni gradient of soil 1 to 6, as no trends in plant growth or shoot dry weight on the different soils could be detected. Even if no gradient in shoot biomass was observed -following the soil mixing gradients- the highest average shoot biomass resulted in soils 6 and LS, significantly higher than in soil 1 (Figure 8 a). Nutrient supply is one possibility as an explanation for the growth differences, as Olsen-P values increased from soil 1 to soil 6 (Table 4). In contrast, soil LS had the second highest average biomass and the lowest Olsen-P values. Furthermore, the TNb values of the pore water also showed no significant differences between the soils throughout the experiment (Figure 18 Supplementary Material).

Nickel hyperaccumulation was confirmed with shoot Ni concentrations well above the Ni hyperaccumulation threshold of 1000 µg g^{-1} in dry shoot weight (Baker and Brooks, 1989; van der Ent et al., 2013) and comparable with previous experimental work on this plant species (Bani et al., 2015a; Bani et al., 2015b; Hipfinger et al., 2022; Rosenkranz et al., 2019; Tognacchini et al., 2020). The highest Ni content was observed in soil 6 and soil LS, significantly higher than all the other soils except for soil 3 (Figure 9 c) and those were as well the soils with the highest plant biomass (Figure 8) resulting in the highest Ni yields. Although no Fe deficiency symptoms

appeared during the experiment, Fe concentrations in shoots were critically low as they range from 41 (soil LS) to 62 (soil 3) mg kg^{-1} DW (Figure 9, Table 5 Supplementary Material). In comparison Tognacchini et al. (2020) reported 189 mg kg^{-1} Fe in DW of *O. chalcidica* shoots grown on ultramafic soil from the field. Phosphorous in shoots was in a comparable range for soils 1 to 6 but showed significantly higher concentrations for soil LS (Figure 9), although soil LS had Olsen-P values that were at least three times lower than for soil 1 to 6 in planted pots after the pot experiment (Table 6, Supplementary Material).

7.3 Effects of the experimental design

The pore water pH and most of the ionome of control pots remained stable throughout the experiment, indicating that no process was strongly affecting the soil environment originating from the experimental design (Figure 13, Figure 14, Figure 15 and Figure 16) Only total N in pore water was significantly lower in control pots of soil 1 to 4 during the pot experiment (Figure 18 Supplementary Material). Maintaining 60% WHC of the control pots by watering perhaps resulted in enhanced microbial activity that consumed N and reduced available N concentrations in pore water. Another observation was that soil pH decreased by 0.2 – 0.4 values comparing control pots after the experiment to the initial soil characterisation before the experiment (Table 4, Table 6 Supplementary Material). Furthermore a slight increase of the labile Ni fractions (DTPA- and $Sr(NO_3)_2$-extractable Ni) in control pots was observed. This was presumably caused as well by microbial activity that was promoted with the daily watering of the soils and resulted in enhanced mineral dissolution and degradation of organic matter that could lead to a decrease in pH and increase in labile Ni.

7.4 Indications for root exudation of O. chalcidica

The rhizosphere of hyperaccumulator plants has long been poorly understood and there has been little knowledge of how those plants influence their soil environment. In this study we found indications for root exudation of *O. chalcidica* during hyperaccumulation of Ni. The strong DOC increase in planted compared with unaffected concentrations in the controls (Figure 16) suggests that root exudation of low molecular weight compounds was contributing to increased organic carbon content in pore water. Recent findings of Álvarez-López et al. (2021) suggest that the Ni hyperaccumulator *O. serpyllifolia* actively increases Ni solubility in the rhizosphere. However, they conclude in their study that this was rather a consequence of the plant's effort to improve nutrient status through enhanced mineral weathering by root exudation than a foraging for Ni (Álvarez-López et al., 2021). They found an increase in DOC in the rhizosphere of field-grown *O. serpyllifolia* compared to bulk soil and an excluder species,

which seemed to be caused by roots of the hyperaccumulator (Álvarez-López et al., 2021). Similar observations have already been made for other hyperaccumulator plants such as by Wenzel et al. (2003) and Puschenreiter et al. (2003; 2005) for *N. goesingensis* who recorded increased DOC concentrations and suggested that root exudates accounted for this. Likewise in the present study a strong and significant increase of DOC in pore water in planted pots compared to control pots suggest that *O. chalcidica* was altering the rhizosphere by root exudation of organic compounds. So far, there have been very few studies focusing on root processes from this plant and these data show that there are first indicators of active root exudation from this hyperaccumulator.

7.5 Root-induced effects on rhizosphere soil

Alkalinisation of soil and pore water pH was one significant observation of root-induced changes by *O. chalcidica* and is well in line with previous findings of Wenzel et al. (2003) who observed an increase in rhizosphere pH of field-grown *N. goesingensis* from the same serpentine area from which the soil samples for this study were taken. Several studies also observed an alkalinisation of soil pH in the rhizosphere during hyperaccumulation of Ni (e.g. Álvarez-López et al., 2021; Puschenreiter et al., 2005,) and evidence increases that this is the common strategy of Ni hyperaccumulator plants to alter their root environment. There is further experimental work where an increase in soil pH was associated with an increase in foliar Ni concentrations (Everhart et al., 2006; Kukier et al., 2004; Li et al., 2003b). However, it is not fully understood what causes rhizosphere alkalinisation. Wenzel et al. (2003) suggested that ligand-induced dissolution of orthosilicates according to (2) (Furrer and Sticher, 2014), could explain the increase in soil pH.

$$Mg_2SiO_4 + 16\,H_2O \leftrightarrow 2\,Mg(H_2O)_6^{2+} + Si(OH)_4 + 4\,OH^- \quad (2)$$

In the present study just limited evidence for enhanced, root-induced mineral dissolution could be detected. Iron solubilisation increased as pore water Fe concentration raised in planted pots (Figure 15 c, d) and labile Fe was slightly but not significant higher in planted pots after the pot experiment (Table 6 Supplementary Material). However, unpublished results of Tognacchini et al (2022) showed that *O. chalcidica* substantially increased pH of a root sampling solution (1 mg/l Micropur in HQ water) within a few hours when grown hydroponically, suggesting that the alkalinisation is not originating from mineral dissolution but from other plant-induced processes. One explanation for this observation could be a direct release of OH^- ions by the roots (Hinsinger et al., 2003) that immediately would have an effect of soil solution pH.

Another option discussed in literature about rhizosphere alkalinisation would be a regulation of the cation-anion exchange balance by the plant (Hinsinger et al., 2003). As N is the element that is taken up at the highest ratio for plants (Kirkby, 2012) and is present in well oxidised soils in the form of NO_3^{2-}, the charge imbalance of an excess of anions is compensated by taking up higher amounts of H^+ by plants (Gahoonia et al., 1992; Hinsinger et al., 2003). Subsequently, rhizosphere pH would increase if H^+ is removed from soil solution. Likewise we also found a strong depletion of the total N in pore water of planted pots during the pot experiment (Figure 18, Supplementary Material). In a study investigating Cd/Zn hyperaccumulation Luo et al. (2000) observed an alkalinisation of rhizosphere pH of *N. caerulescens* and suggested that a charge balance in the plant cells was responsible for the pH increase.

The influence of an increase in soil pH on Ni hyperaccumulation of *O. chalcidica* and *O. corsica* (both former *Alyssum*) was studied in more detail by Li et al. (2003b). They were the first to describe an increase in Ni hyperaccumulation as pH was increased by liming (Li et al., 2003b). Similar observations have been made recently by Ghafoori et al. (2022) who investigated three *Odontarrhena* species from Iranian serpentine regions and reported significant positive correlations between Ni concentration in the shoots and soil pH. They proposed that through evolutionary adaptations to ultramafic high pH soils, the uptake of nickel via transporters into the root is reduced when the soil pH is decreased (Ghafoori et al., 2022). In return this suggested that an increase of pH around the root would facilitate the uptake of Ni and other essential nutrients that are channelled through root cation transporters (Li et al., 2003b).

Furthermore, van der Ent et al. (2016) found that Ni hyperaccumulators in Sabah (Malaysia) consistently grew on soils with pH > 6.3 and high concentrations of phytoavailable concentrations of Ca, Mg and Ni. Higher pH values of ultramafic soils could favour basiphilous plants and could give hyperaccumulators an advantage over acidophilic plants under these circumstances (Ghafoori et al., 2022). In the same study van der Ent et al. (2016) gave three possible explanations that are also in agreement with Li et al. (2003b) and suggest why it is advantageous for hyperaccumulators to increase the pH around the root: 1. Rhizosphere alkalinisation could provide higher stability of Ni-amino acid complexes and other organic ligands (van der Ent et al., 2016). 2. Sorption upon CEC is in general pH dependent and could enhance when pH is increasing and 3. increased surface complexation of Ni at Fe oxides (van der Ent et al., 2016). Concerning the higher stability of Ni-organic ligands, especially amino acids that are important for hyperaccumulation like histidine and phenols appear to be more stable as pH increases (Pyreu and Nikitina, 2021). In any case, as a result of one or more of these processes, a strong increase in soil and pore water pH was observed that was accompanied by a similar increase in pore water Ni concentrations (Figure 13 and Figure 14). However, the

correlations between the increase in Ni of the pore water T_3 concentrations and the increase in pH were positive but rather low for both pH of the pore water T_3 (R^2 = 0.43, Figure 17) and soil pH (R^2 = 0.41, Figure 17).

Another increase coinciding with Ni, pH and Fe in the pore water was observed for DOC concentrations for T_2 and T_3. Furthermore, a highly significant positive correlations between the increase in pore water DOC and Ni (R^2 = 0.96, Figure 17) as well as Fe (R^2 = 0.86, Figure 17) was found in this study for T_3. Those findings are well in agreement with those of Wenzel et al. (2003) who reported a significant correlation (R^2 = 0.85) between DOC and Ni from soil solution of the hyperaccumulator *N. goesingensis*. By running biogeochemical modelling Wenzel et al. (2003) proved that an increase in Ni solubility in the rhizosphere of *N. goesingensis* facilitated an increased formation of Ni-dissolved organic matter (DOM) complexes. Additionally, increasing pH showed to increase the stability of Ni-DOM complexes (Everhart et al., 2006; Kukier and Chaney, 2001), which also occurred in this study as mentioned above. Those observations strongly suggest that the amount and quality of DOC in soil can largely influence the mobility and bioavailability of Ni in soil (Wenzel et al., 2018). The role of DOC in activating Cd and Zn in the rhizosphere of the hyperaccumulator *Sedum alfredii* was investigated in more detail by Li et al. (2011; 2012). Li et al. (2012) found elevated DOM concentrations in rhizosphere soil from a hyperaccumulator ecotype compared to a non-hyperaccumulator ecotype. Rhizosphere from the hyperaccumulator contained not only 34% more DOM but also the DOM consisted of markedly higher hydrophilic fractions that are able to chelate metals and reduced sorption of Zn to minerals in soil (Li et al., 2012). This could be one important mechanism by which hyperaccumulator plants mobilise metals in the rhizosphere and the present study provides first indication of similar processes for Ni hyperaccumulation of *O. chalcidica*. Further research characterising the composition of DOC in the rhizosphere of *O. chalcidica* grown on ultramafic soils are the next step to decipher which substances are exuded by hyperaccumulator plants and how they mobilise Ni.

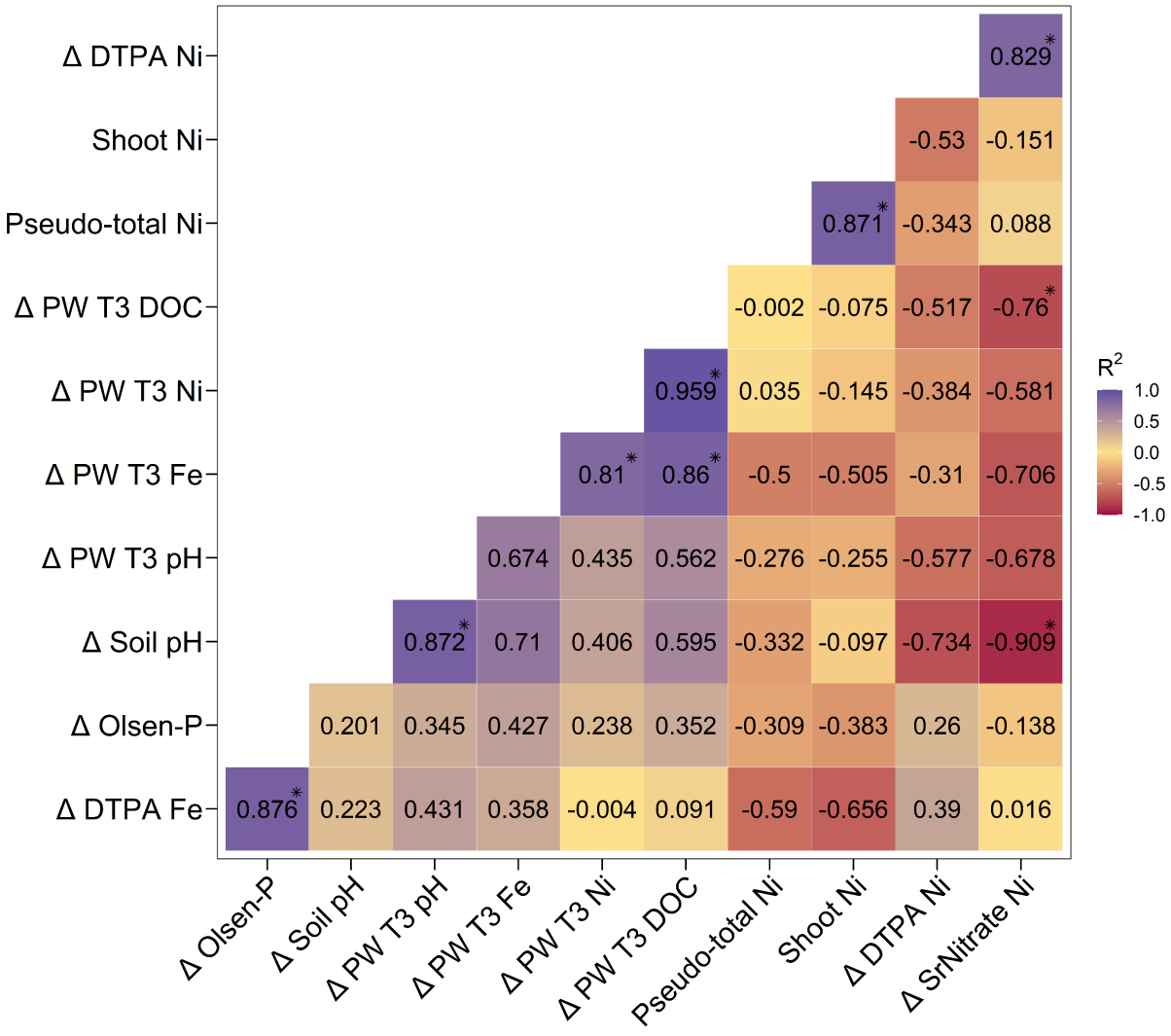

Figure 17: Correlation matrix of selected variables from the pot experiment. Values presented are R^2 resulting from Pearson's r with $p < 0.05$. Significant values are marked with asterisks. The considered variables are the differences between planted and control pots (Δ) of the extractions Olsen-P, DTPA and $Sr(NO_3)_2$ (=Sr) and pH after the pot experiment, Δ between planted and control of the pore water (PW) T_3 Ni, Fe, and DOC concentrations as well as pH and the pseudo-total (AR) Ni and shoot dry weight (DIG) Ni concentrations. The Δ values for a change between planted and control pots were used to prevent a bias of the correlation due to the mixing of the soil gradient.

7.6 Non-linear relationship between plant and soil Ni

One hypothesis of this study was that due to mobilisation of Ni in the rhizosphere shoot Ni concentrations in *O. chalcidica* would not follow the linear soil Ni concentrations of the soil mixing scheme (Table 1). Although plant Ni concentrations did not follow the same linear trend as pseudo-total Ni in soil, lowest Ni concentrations have resulted in soil 1 and the highest in soil 6 and LS (Figure 9 c). Rather, it seems that a "double linearity" has developed with increasing Ni from soil 1 to 3 and again from soil 4 to 6. Furthermore, a positive and significant correlation between plant Ni and pseudo-total Ni was found (R^2 = 0.87, Figure 17). Interestingly, no significant correlations between plant Ni and labile soil Ni were found. In fact, the best correlation has resulted between the reduction of DTPA-extractable Ni of planted pots and shoot Ni having a correlation coefficient of R^2 = -0.53 (Figure 17). There are contrasting results about

correlations of soil labile Ni and shoot Ni concentrations in literature. This could be due to the fact that hyperaccumulators may not only take up Ni from the soil labile pool but access Ni from non-labile pool as well (Álvarez-López et al., 2021). The indications of the present study regarding root exudation of *O. chalcidica* during Ni hyperaccumulation support the hypothesis that hyperaccumulator plants could actively alter the soil chemical equilibrium so that more Ni is replenished from the non-labile pool. This could further explain why plant Ni is also correlating better with soil pseudo-total Ni than the soil labile Ni pool (Figure 17). The results of soil LS are particularly interesting in this regard because both DTPA- and $Sr(NO_3)_2$-extractable Ni were three times lower in soil LS than in soil 6 but plant Ni compared well between the two soils (Table 5, Table 6, Supplementary Material). This reveals that soil LS was more efficient in mobilising Ni, possibly by root exudation after excessive plant uptake. Since soil LS also had by far the highest pH value, the pH dependence of Ni uptake effectiveness described in the previous chapter (7.5) could be a supporting explanation for this.

In addition, hyperaccumulators preferably extract Ni from higher labile forms of Ni-bearing phases (e.g. smectite) rather than from less labile ones (e.g. chrysotile) (Centofanti et al., 2012; Montargès-Pelletier et al., 2008). To cover the plants' full uptake capacity the amount of available Ni from more easily mobilizable pools may not be sufficient and less labile pools have to be assessed by rhizosphere processes. Hence depending on the soil composition and Ni bearing phases, plant uptake relates differently to soil Ni labile phases. These results showed that the effectiveness of Ni uptake depends not only on the total and labile Ni concentrations in soil but relates also to other important soil physiochemical parameters, especially soil pH.

7.7 Changes in Ni-, Fe- and P availability

Iron oxides are considered to be one of the most important mineral phases for containing significant amounts of Ni and P in ultramafic soil surface horizons (Cheng et al., 2011; Gasparatos and Barbayiannis, 2019) and therefore this study aims to investigate how the three elements behave when Ni availability is altered by *O. chalcidica* during hyperaccumulation. Both assessments for the labile Ni pool (DTPA and $Sr(NO_3)_2$) showed a significant decrease in available Ni concentrations of planted pots after the pot experiment (Figure 10 a, b). It is assumed that the labile Ni pool is depleted during hyperaccumulation by excessive uptake of Ni, thus shifting the chemical equilibrium of Ni in the soil (Centofanti et al., 2012; Wenzel et al., 2003). This can partly explain the reduction of the labile pool in the soil. However, the differences in DTPA-extractable Ni removed by plant uptake between planted and unplanted pots can only account for 40-70% of the total Ni depletion in soil. For instance in the case of soil 6 one plant extracted around 7 mg $plant^{-1}$ Ni (Table 5, Supplementary Material), whereas the

difference in DTPA-extractable Ni for this soil was around 14 mg pot^{-1} between planted and unplanted pots (Table 6, Supplementary Material, values normalised to 450/550 g of soil in pots). Therefore an additional process next to plant uptake might have been responsible for the decreased labile pool during the pot experiment. A bias of the values by the pore water sampling can be neglected, because in the course of four samplings 40 ml soil solution was removed which accounted for roughly 0.02 mg Ni per pot. Various works on ultramafic soils where soil pH was artificially changed showed a decrease in DTPA or $Sr(NO_3)_2$-extractable Ni as soil pH increased and vice versa (Everhart et al., 2006; Kukier et al., 2004; Kukier and Chaney, 2001; Robinson et al., 1999). So, there is a pH effect that decreases labile Ni when soil pH increases. This is supported by the fact that soil LS of the pot experiment was the only soil with a difference in labile Ni that can be completely explained by plant uptake (Δ DTPA $_{control - planted}$ = 2.8 mg pot^{-1}, plant uptake 5.8 mg $plant^{-1}$ Ni, Table 6, Supplementary Material) and concomitantly was the only soil where no significant difference in soil pH between planted and unplanted pots was detected (Table 5, Supplementary Material). For this soil plant uptake is even by a factor of two higher than the depletion in DTPA-extractable Ni, showing that a resupply from the non-labile pool had to compensate the excessive uptake. Further confirmation of the pH effect was found in this study as a highly significant correlation between the reduction in $Sr(NO_3)_2$-extractable Ni and the increase in pH with R^2 = -0.91 (Figure 17) and a high but not significant correlation between the reduction of DTPA-extractable Ni and the increase in pH (R^2 = -0.73, Figure 17). That pH dependent decrease in Ni availability could perhaps be related to the in chapter 7.5 mentioned higher stability of Ni-SOM complexes with increasing pH (Everhart et al., 2006; Kukier and Chaney, 2001). SOM however is likely to play the most important role in short term complexation reactions (Shi et al., 2012). Nickel therefore is more stable bound or precipitates on mineral surfaces as soil pH increases (Shi et al., 2012) leading to a reduction in DTPA/$Sr(NO_3)_2$-extractable Ni as observed in the pot experiment of this study. By removing exchangeable Ni from the soil solution, the chemical equilibrium in the soil shifts accordingly, allowing an increased desorption of Ni (Wenzel et al., 2003) . This newly desorbed Ni is rather in ionic form or complexed by simple ligands and therefore excessive Ni can be taken up by the hyperaccumulator plants (He et al., 2012; Kabata-Pendias, 2011). This process could as well be reflected in the pot experiment by the highly elevated Ni concentrations in pore water (Figure 14).

Together with Ni also large quantities of Fe became soluble, resulting in highly elevated Fe concentrations in pore water (Figure 15) that furthermore correlated significantly with both Ni (R^2 = 0.81, Figure 17) and DOC (R^2 = 0.86, Figure 17) in pore water. Therefore, it can be assumed that by root exudation of organic ligands from *O. chalcidica* Ni and Fe get solubilised. This is

remarkable since Fe is commonly mobilised by strategy I plants (most plants except of grasses) via a release of H^+ resulting in a reductive dissolution of Fe^{III}-bearing minerals in the rhizosphere (Hinsinger et al., 2003; Marschner and Römheld, 1994). Although this strong solubilisation of Fe is visible in pore water samples, Fe concentrations in shoots of *O. chalcidica* showed low to deficient values (Figure 15, Figure 9 b) and it is apparent that the plants struggled to take up Fe. Competition in the uptake of Fe due to the very high Ni concentrations in the pore water could be the reason for this, as both cations probably share the same transporter into the root cell (Nishida et al., 2011; van der Pas and Ingle, 2019). Regarding the Fe availability assessed by DTPA/$Sr(NO_3)_2$ extractions, only slightly increased concentrations were measured on average for the planted pots compared to controls but there was no statistical significance for any of the soils (Table 6, Supplementary Material). However, a significant correlation between the differences in DTPA-extractable Fe of planted and control pots and the increase in Olsen-P values was detected ($R^2 = 0.88$, Figure 17). This suggests that P is also co-mobilised with Ni and Fe and therefore P availability as well increased. However, P values in pore water could not be reliably assessed, as the concentrations were below the quantification limit (20 µg l^{-1}) for the majority of the samples. This could indicate that available P is directly taken up by the plants since hyperaccumulator plants are well adapted to nutrient poor ultramafic soils (Proctor and Woodell, 1975) and perhaps have effective P uptake mechanisms. Soil LS showed to have the highest effectiveness in P uptake because P shoot concentrations were comparable with soils 1 to 6 (Figure 9 a) but Olsen-P values three times lower (Table 6 Supplementary Material). This might be explained by weaker binding of P at higher pH values of soil LS as the release kinetics of P could be enhanced compared to soil 1 to 6. Furthermore, the Olsen-P single extraction does not include desorption kinetics in its method and P resupply could be high for soil LS and compensate for the lower bioavailable fraction when P is quickly replenished after depletion of the labile pool.

7.8 Differences of Ni bioavailability methods

Ni bioavailability was assessed by two different methods, single extractions with DTPA and $Sr(NO_3)_2$ as well as determination of dissolved Ni in pore water. Although these methods attempt to observe changes in Ni availability during hyperaccumulation, they sometimes come to different results, or to results that require further interpretation. Hence DTPA and $Sr(NO_3)_2$-extractable Ni decreased in planted pots whereas pore water Ni concentrations increased during the pot experiment. Equilibrium based single batch extraction of phytoavailability for trace metals often showed to be only poorly correlated with plant uptake (Menzies et al., 2007; Puschenreiter et al., 2013) and this study also only found very weak correlations between DTPA

and $Sr(NO_3)_2$ Ni and plant Ni. Although these methods may be useful for non-hyperaccumulator plants, the results of this study indicate that hyperaccumulator plants may access non-labile Ni pools and therefore bioavailability is not sufficiently assessed.

The extractions resemble the soil fraction available for uptake of trace metals into the plant, which is limited by the plant uptake mechanism (internalisation), but studies showed that diffusive transport to the root surface is rather the uptake limitation for trace metals (Degryse et al., 2009). This is particularly important for hyperaccumulators, as these take up trace metals in exceptionally high quantities, so that replenishment from the solid phase into soil solution must compensate the uptake by the plants (Álvarez-López et al., 2021). So one of the key questions for estimating Ni bioavailability for hyperaccumulator plants is whether Ni uptake is diffusion or internalisation limited. Alternative methodologies such as the Diffusive Gradient in Thin films (DGT) technique have been shown to correlate better with plant uptake, as they take into account not only the removal of metals from the soil solution but also the subsequent resupply of ions from solid phase, simulating a plant root (Ernstberger et al., 2005; Puschenreiter et al., 2013). Further work on this topic should include techniques like DGT to further elucidate the biogeochemical processes involved in mobilisation and uptake of Ni by hyperaccumulator plants.

8 Conclusion

This study presents the first indication for root exudation of the Ni hyperaccumulator plant *O. chalcidica*, which is a promising candidate for phytomining. It was demonstrated in a pot experiment with increasing Ni gradient that *O. chalcidica* increased concentrations of Ni, Fe and DOC in pore as well as soil and pore water pH. Strong and significant correlations between the increase in Ni, Fe and DOC suggest that exudation of organic low molecular weight compounds are responsible for mobilising Ni and Fe in the rhizosphere. It was assumed that also P would be mobilised along with Ni and Fe, however most P pore water values were below the limit of quantification as P was perhaps immediately taken up by the plants and removed from soil solution. Ni concentrations in soil showed to be an important factor controlling the phytoextraction in *O. chalcidica*, as lowest shoot Ni concentrations were found on soils with lower Ni content and highest shoot Ni concentrations in soils with higher Ni content. In contrast, no significant correlations between DTPA- or $Sr(NO_3)_2$-extractable Ni and shoot Ni was found, suggesting that the soil labile Ni pools assessed by these methods is not a good indicator for plant Ni. Therefore, pseudo-total concentrations seemed to be the more important variable when correlating with plant Ni since *O. chalcidica* is discussed to access the non-labile pool during hyperaccumulation. These findings help to better understand the rhizosphere

processes of Ni hyperaccumulator plants and thereby improve phytomining and advance an alternative method for recycling Ni from soils that are otherwise difficult and laborious to use.

9 References

Alexander, E.B., 2004. Serpentine soil redness, differences among peridotite and serpentinite materials, Klamath Mountains, California. International Geology Review 46 (8), 754–764.

Al-Shehbaz, I.A., 1987. The genera of Alysseae (Cruciferae, Brassicaceae) in the southeastern United States. Journal of the Arnold Arboretum 68 (2), 185–240.

Álvarez-López, V., Puschenreiter, M., Santner, J., Lehto, N., Prieto-Fernández, Á., Wenzel, W.W., Monterroso, C., Kidd, P.S., 2021. Evidence for nickel mobilisation in rhizosphere soils of Ni hyperaccumulator Odontarrhena serpyllifolia. Plant Soil 464 (1-2), 89–107.

Baker, A., Brooks, R.R., 1989. Terrestrial Higher Plants which Hyperaccumulate Metallic Elements - A Review of their Distribution Ecology and Phytochemistry. Biorecovery 1, 81–126.

Baker, A.J.M., 1981. Accumulators and excluders-strategies in the response of plants to heavy metals. Journal of plant nutrition 3 (1-4), 643–654.

Bani, A., Echevarria, G., Montargès-Pelletier, E., Gjoka, F., Sulçe, S., Morel, J.L., 2014. Pedogenesis and nickel biogeochemistry in a typical Albanian ultramafic toposequence. Environmental monitoring and assessment 186 (7), 4431–4442.

Bani, A., Echevarria, G., Sulçe, S., Morel, J.L., 2015a. Improving the Agronomy of Alyssum murale for Extensive Phytomining: A Five-Year Field Study. International journal of phytoremediation 17 (1-6), 117–127.

Bani, A., Echevarria, G., Zhang, X., Benizri, E., Laubie, B., Morel, J.L., Simonnot, M.-O., 2015b. The effect of plant density in nickel-phytomining field experiments with Alyssum murale in Albania. Aust. J. Bot. 63 (2), 72.

Baronnet, A., Andreani, M., Grauby, O., Devouard, B., Nitsche, S., Chaudanson, D., 2007. Onion morphology and microstructure of polyhedral serpentine. American Mineralogist 92 (4), 687–690.

Bonifacio, E., Barberis, E., 1999. PHOSPHORUS DYNAMICS DURING PEDOGENESIS ON SERPENTINITE. Soil Science 164 (12), 960–968.

Bonifacio, E., Zanini, E., Boero, V., Franchini-Angela, M., 1997. Pedogenesis in a soil catena on serpentinite in north-western Italy. Geoderma 75 (1), 33–51.

Buée, M., Boer, W. de, Martin, F., van Overbeek, L., Jurkevitch, E., 2009. The rhizosphere zoo: An overview of plant-associated communities of microorganisms, including phages,

bacteria, archaea, and fungi, and of some of their structuring factors. Plant Soil 321 (1-2), 189–212.

Caillaud, J., Proust, D., Philippe, S., Fontaine, C., Fialin, M., 2009. Trace metals distribution from a serpentinite weathering at the scales of the weathering profile and its related weathering microsystems and clay minerals. Geoderma 149 (3-4), 199–208.

Caillaud, J., Proust, D., Righi, D., 2006. Weathering sequences of rock-forming minerals in a serpentinite: influence of microsystems on clay mineralogy. Clays and Clay Minerals 54 (1), 87–100.

Caillaud, J., Proust, D., Righi, D., Martin, F., 2004. Fe-Rich Clays in a Weathering Profile Developed from Serpentinite. Clays and Clay Minerals 52 (6), 779–791.

Cappa, J.J., Pilon-Smits, E.A., 2014. Evolutionary aspects of elemental hyperaccumulation. Planta 239 (2), 267–275.

Carter, M.R., Gregoric, E.G. (Eds.), 2008. Soil Sampling and Methods of Analysis 2. Taylor & Francis.

Centofanti, T., Siebecker, M.G., Chaney, R.L., Davis, A.P., Sparks, D.L., 2012. Hyperaccumulation of nickel by Alyssum corsicum is related to solubility of Ni mineral species. Plant Soil 359 (1), 71–83.

Chaney, R.L., 2018. Phytoextraction and phytomining of soil nickel, in: Tsadilas, C., Rinklebe, J., Selim, M., Eds (Ed.), Nickel in Soils and Plants. CRC Press, pp. 341–374.

Chaney, R.L., Baker, A.J.M., Morel, J.L., 2021. The Long Road to Developing Agromining/Phytomining, in: van der Ent, A., Baker, A.J., Echevarria, G., Simonnot, M.-O., Morel, J.L. (Eds.), Agromining: Farming for Metals: Extracting Unconventional Resources Using Plants. Springer International Publishing, Cham, pp. 1–22.

Chardot, V., Echevarria, G., Gury, M., Massoura, S., Morel, J.L., 2007. Nickel bioavailability in an ultramafic toposequence in the Vosges Mountains (France). Plant Soil 293 (1), 7–21.

Chardot-Jacques, V., Calvaruso, C., Simon, B., Turpault, M.-P., Echevarria, G., Morel, J.-L., 2013. Chrysotile dissolution in the rhizosphere of the nickel hyperaccumulator Leptoplax emarginata. Environmental science & technology 47 (6), 2612–2620.

Cheng, C.-H., Jien, S.-H., Iizuka, Y., Tsai, H., Chang, Y.-H., Hseu, Z.-Y., 2011. Pedogenic Chromium and Nickel Partitioning in Serpentine Soils along a Toposequence. Soil Science Society of America Journal 75 (2), 659–668.

Clemens, S., 2006. Toxic metal accumulation, responses to exposure and mechanisms of tolerance in plants. Biochimie 88 (11), 1707–1719.

Clemens, S., Palmgren, M.G., Krämer, U., 2002. A long way ahead: understanding and engineering plant metal accumulation. Trends in Plant Science 7 (7), 309–315.

Dalton, D.A., 2018. Essentiality of Nickel for Plants. In: Nickel in Soils and Plants; Tsadilas, C., Rinklebe, J., Selim, M., Eds, 1–20.

Degryse, F., Smolders, E., Zhang, H., Davison, W., 2009. Predicting availability of mineral elements to plants with the DGT technique: a review of experimental data and interpretation by modelling. Environmental Chemistry 6 (3), 198–218.

Deng, T.-H.-B., van der Ent, A., Tang, Y.-T., Sterckeman, T., Echevarria, G., Morel, J.-L., Qiu, R.-L., 2018. Nickel hyperaccumulation mechanisms: a review on the current state of knowledge. Plant Soil 423 (1-2), 1–11.

Dixon, N.E., Gazzola, C., Blakeley, R.L., Zerner, B., 1975. Jack bean urease (EC 3.5.1.5). Metalloenzyme. Simple biological role for nickel. Journal of the American Chemical Society 97 (14), 4131–4133.

Dudley, T.R., 1964. Studies in Alyssum: Near Eastern representatives and their allies, I. Journal of the Arnold Arboretum 45 (1), 57–100.

Echevarria, G., 2021. Genesis and Behaviour of Ultramafic Soils and Consequences for Nickel Biogeochemistry, in: van der Ent, A., Baker, A.J., Echevarria, G., Simonnot, M.-O., Morel, J.L. (Eds.), Agromining: Farming for Metals. Mineral Resource Reviews. Springer International Publishing, Cham, pp. 215–238.

Echevarria, G., Massoura, S.T., Sterckeman, T., Becquer, T., Schwartz, C., Morel, J.L., 2006. Assessment and control of the bioavailability of nickel in soils. Environmental toxicology and chemistry 25 (3), 643–651.

Ernstberger, H., Zhang, H., Tye, A., Young, S., Davison, W., 2005. Desorption Kinetics of Cd, Zn, and Ni Measured in Soils by DGT. Environmental science & technology 39 (6), 1591–1597.

Eskew, D.L., Welch, R.M., Cary, E.E., 1983. Nickel: an essential micronutrient for legumes and possibly all higher plants. Science 222 (4624), 621–623.

Everhart, J.L., McNear, D., Peltier, E., van der Lelie, D., Chaney, R.L., Sparks, D.L., 2006. Assessing nickel bioavailability in smelter-contaminated soils. Science of The Total Environment 367 (2), 732–744.

Flora of North America Association, 2010. Flora of North America. Volume 7: Brassicaceae. Flora of North America Association. http://floranorthamerica.org/Alyssum_murale. Accessed 5 August 2022.

Fritsch, E., Balan, E., Petit, S., Juillot, F., 2021. Structural, textural, and chemical controls on the OH stretching vibrations in serpentine-group minerals. Eur. J. Mineral. 33 (4), 447–462.

Furrer, G., Sticher, H., 2014. Chemische Verwitterungsprozesse, in: Blume, H.-P., Stahr, K., Fischer, W., Guggenberger, G., Horn, R., Frede, H.-G., Felix-Henningsen, P. (Eds.), Handbuch der Bodenkunde. Wiley, pp. 1–18.

Gahoonia, T.S., Claassen, N., Jungk, A., 1992. Mobilization of phosphate in different soils by ryegrass supplied with ammonium or nitrate. Plant Soil 140 (2), 241–248.

García de la Torre, Majorel-Loulergue, C., Rigaill, G.J., Alfonso-González, D., Soubigou-Taconnat, L., Pillon, Y., Barreau, L., Thomine, S., Fogliani, B., Burtet-Sarramegna, V., Merlot, S., 2020. Wide cross-species RNA-Seq comparison reveals convergent molecular mechanisms involved in nickel hyperaccumulation across dicotyledons. The New phytologist 229 (2), 994–1006.

Gasparatos, D., Barbayiannis, N., 2019. The Origin of Nickel in Soils, in: Tsadilas, C.D., Rinklebe, J., & Selim, H.M. (Ed.), Nickel in Soils and Plants. CRC Press, pp. 105–128.

Ghaderian, S.M., Ghasemi, R., Hajihashemi, F., 2015. Interaction of nickel and manganese in uptake, translocation and accumulation by the nickel-hyperaccumulator plant, Alyssum bracteatum (Brassicaceae). Aust. J. Bot. 63 (2), 47.

Ghafoori, M., Shariati, M., van der Ent, A., Baker, A.J.M., 2022. Nickel hyperaccumulation, elemental profiles and agromining potential of three species of Odontarrhena from the ultramafics of Western Iran. International journal of phytoremediation, 1–12.

Gonnelli, C., Renella, G., 2013. Chromium and Nickel, in: Alloway, B.J. (Ed.), Heavy Metals in Soils, vol. 22. Environmental Pollution. Springer Netherlands, Dordrecht, pp. 313–333.

Guillot, S., Hattori, K., 2013. Serpentinites: essential roles in geodynamics, arc volcanism, sustainable development, and the origin of life. Elements 9 (2), 95–98.

Hall, J.á., 2002. Cellular mechanisms for heavy metal detoxification and tolerance. Journal of experimental botany 53 (366), 1–11.

Haydon, M.J., Cobbett, C.S., 2007. Transporters of ligands for essential metal ions in plants. New phytologist 174 (3), 499–506.

He, S., He, Z., Yang, X., Baligar, V.C., 2012. Chapter Three - Mechanisms of Nickel Uptake and Hyperaccumulation by Plants and Implications for Soil Remediation, in: Sparks, D.L. (Ed.), Advances in Agronomy, vol. 117. Academic Press, pp. 117–189.

Hiltner, L., 1904. Uber nevere Erfahrungen und Probleme auf dem Gebiet der Boden Bakteriologie und unter besonderer Beurchsichtigung der Grundungung und Broche. Arbeit. Deut. Landw. Ges. Berlin 98, 59–78.

Hinsinger, P., Gobran, G.R., Gregory, P.J., Wenzel, W.W., 2005. Rhizosphere geometry and heterogeneity arising from root-mediated physical and chemical processes. New phytologist 168 (2), 293–303.

Hinsinger, P., Plassard, C., Tang, C., Jaillard, B., 2003. Origins of root-mediated pH changes in the rhizosphere and their responses to environmental constraints: A review. Plant Soil 248 (1), 43–59.

Hipfinger, C., Laux, M., Puschenreiter, M., 2022. Comparison of four nickel hyperaccumulator species in the temperate climate zone of Central Europe. Journal of Geochemical Exploration 234, 106933.

Hirsch, P.R., Miller, A.J., Dennis, P.G., 2013. Do root exudates exert more influence on rhizosphere bacterial community structure than other rhizodeposits? Molecular microbial ecology of the rhizosphere 1, 229–242.

Hseu, Z.Y., Tsai, H., Hsi, H.C., Chen, Y.C., 2007. Weathering sequences of clay minerals in soils along a serpentinitic toposequence. Clays and Clay Minerals 55 (4), 389–401.

Hseu, Z.-Y., Chen, Z.-S., Tsai, C.-C., Jien, S.-H., 2016. Portable X-Ray Fluorescence (pXRF) for Determining Cr and Ni Contents of Serpentine Soils in the Field, in: Hartemink, A.E., Minasny, B. (Eds.), Digital Soil Morphometrics. Springer International Publishing, Cham, pp. 37–50.

Hseu, Z.-Y., Zehetner, F., Fujii, K., Watanabe, T., Nakao, A., 2018. Geochemical fractionation of chromium and nickel in serpentine soil profiles along a temperate to tropical climate gradient. Geoderma 327, 97–106.

Ingle, R.A., Mugford, S.T., Rees, J.D., Campbell, M.M., Smith, J.A.C., 2005. Constitutively High Expression of the Histidine Biosynthetic Pathway Contributes to Nickel Tolerance in Hyperaccumulator Plants. The Plant Cell 17 (7), 2089–2106.

Isnard, S., L'huillier, L., Rigault, F., Jaffré, T., 2016. How did the ultramafic soils shape the flora of the New Caledonian hotspot? Plant Soil 403 (1), 53–76.

Jones, D.L., 1998. Organic acids in the rhizosphere – a critical review. Plant Soil 205 (1), 25–44.

Kabata-Pendias, A., 2011. Trace Elements in Soils and Plants: Chapter 15: Elements of Group 10. CRC Press.

Kazakou, E., Dimitrakopoulos, P.G., Baker, A.J., Reeves, R.D., Troumbis, A.Y., 2008. Hypotheses, mechanisms and trade-offs of tolerance and adaptation to serpentine soils: from species to ecosystem level. Biological Reviews 83 (4), 495–508.

Kelley, D.S., Karson, J.A., Früh-Green, G.L., Yoerger, D.R., Shank, T.M., Butterfield, D.A., Hayes, J.M., Schrenk, M.O., Olson, E.J., Proskurowski, G., Jakuba, M., Bradley, A., Larson, B., Ludwig, K., Glickson, D., Buckman, K., Bradley, A.S., Brazelton, W.J., Roe, K., Elend, M.J., Delacour, A., Bernasconi, S.M., Lilley, M.D., Baross, J.A., Summons, R.E., Sylva, S.P., 2005. A serpentinite-hosted ecosystem: the Lost City hydrothermal field. Science 307 (5714), 1428–1434.

Kerkeb, L., Krämer, U., 2003. The Role of Free Histidine in Xylem Loading of Nickel inAlyssum lesbiacum and Brassica juncea. Plant Physiology 131 (2), 716–724.

Kidd, P., Barceló, J., Bernal, M.P., Navari-Izzo, F., Poschenrieder, C., Shilev, S., Clemente, R., Monterroso, C., 2009. Trace element behaviour at the root–soil interface: Implications in phytoremediation. Environmental and Experimental Botany 67 (1), 243–259.

Kidd, P.S., Bani, A., Benizri, E., Gonnelli, C., Hazotte, C., Kisser, J., Konstantinou, M., Kuppens, T., Kyrkas, D., Laubie, B., Malina, R., Morel, J.-L., Olcay, H., Pardo, T., Pons, M.-N., Prieto-Fernández, Á., Puschenreiter, M., Quintela-Sabarís, C., Ridard, C., Rodríguez-Garrido, B., Rosenkranz, T., Rozpądek, P., Saad, R., Selvi, F., Simonnot, M.-O., Tognacchini, A., Turnau, K., Ważny, R., Witters, N., Echevarria, G., 2018. Developing Sustainable Agromining Systems in Agricultural Ultramafic Soils for Nickel Recovery. Front. Environ. Sci. 6.

Kierczak, J., Neel, C., Bril, H., Puziewicz, J., 2007. Effect of mineralogy and pedoclimatic variations on Ni and Cr distribution in serpentine soils under temperate climate. Geoderma 142 (1), 165–177.

Kirkby, E., 2012. Chapter 1 - Introduction, Definition and Classification of Nutrients, in: Marschner, P. (Ed.), Marschner's Mineral Nutrition of Higher Plants (Third Edition). Academic Press, San Diego, pp. 3–5.

Krämer, U., 2010. Metal hyperaccumulation in plants. Annual review of plant biology 61, 517–534.

Krämer, U., Cotter-Howells, J.D., Charnock, J.M., Baker, A.J.M., Smith, J.A.C., 1996. Free histidine as a metal chelator in plants that accumulate nickel. Nature 379 (6566), 635–638.

Kukier, U., Chaney, R.L., 2001. Amelioration of nickel phytotoxicity in muck and mineral soils. Journal of environmental quality 30 (6), 1949–1960.

Kukier, U., Peters, C.A., Chaney, R.L., Angle, J.S., Roseberg, R.J., 2004. The effect of pH on metal accumulation in two Alyssum species. Journal of environmental quality 33 (6), 2090–2102.

Küpper, H., Lombi, E., Zhao, F.-J., Wieshammer, G., McGrath, S.P., 2001. Cellular compartmentation of nickel in the hyperaccumulators Alyssum lesbiacum, Alyssum bertolonii and Thlaspi goesingense. Journal of experimental botany 52 (365), 2291–2300.

Le Bas, M.J., Streckeisen, A.L., 1991. The IUGS systematics of igneous rocks. Journal of the Geological Society 148 (5), 825–833.

Leigh Broadhurst, C., Tappero, R.V., Maugel, T.K., Erbe, E.F., Sparks, D.L., Chaney, R.L., 2009. Interaction of nickel and manganese in accumulation and localization in leaves of the Ni hyperaccumulators Alyssum murale and Alyssum corsicum. Plant Soil 314 (1-2), 35–48.

Li, T., Di, Z., Yang, X., Sparks, D.L., 2011. Effects of dissolved organic matter from the rhizosphere of the hyperaccumulator Sedum alfredii on sorption of zinc and cadmium by different soils. Journal of Hazardous Materials 192 (3), 1616–1622.

Li, T., Xu, Z., Han, X., Yang, X., Sparks, D.L., 2012. Characterization of dissolved organic matter in the rhizosphere of hyperaccumulator Sedum alfredii and its effect on the mobility of zinc. Chemosphere 88 (5), 570–576.

Li, Y.-M., Chaney, R., Brewer, E., Roseberg, R., Angle, J.S., Baker, A., Reeves, R., Nelkin, J., 2003a. Development of a technology for commercial phytoextraction of nickel: economic and technical considerations. Plant Soil 249 (1), 107–115.

Li, Y.-M., Chaney, R.L., Brewer, E.P., Angle, J.S., Nelkin, J., 2003b. Phytoextraction of nickel and cobalt by hyperaccumulator Alyssum species grown on nickel-contaminated soils. Environmental science & technology 37 (7), 1463–1468.

Lindsay, W.L., Norvell, W.A., 1978. Development of a DTPA Soil Test for Zinc, Iron, Manganese, and Copper. Soil Science Society of America Journal 42 (3), 421–428.

Luo, Y., Christie, P., Baker, A., 2000. Soil solution Zn and pH dynamics in non-rhizosphere soil and in the rhizosphere of Thlaspi caerulescens grown in a Zn/Cd-contaminated soil. Chemosphere 41 (1), 161–164.

Madden, M.S., 1988. Adapting the Sr(NO3)2 method for determining available cations to a routine soil testing procedure. University of Wisconsin--Madison.

Marschner, H., Römheld, V., 1994. Strategies of plants for acquisition of iron. Plant Soil 165 (2), 261–274.

Massoura, S.T., Echevarria, G., Becquer, T., Ghanbaja, J., Leclerc-Cessac, E., Morel, J.-L., 2006. Control of nickel availability by nickel bearing minerals in natural and anthropogenic soils. Geoderma 136 (1), 28–37.

Massoura, S.T., Echevarria, G., Leclerc-Cessac, E., Morel, J.L., 2004. Response of excluder, indicator, and hyperaccumulator plants to nickel availability in soils. Soil Res. 42 (8), 933.

McCollom, T.M., Klein, F., Robbins, M., Moskowitz, B., Berquó, T.S., Jöns, N., Bach, W., Templeton, A., 2016. Temperature trends for reaction rates, hydrogen generation, and partitioning of iron during experimental serpentinization of olivine. Geochimica et Cosmochimica Acta 181, 175–200.

Mellini, M., Trommsdorff, V., Compagnoni, R., 1987. Antigorite polysomatism: behaviour during progressive metamorphism. Contributions to Mineralogy and Petrology 97 (2), 147–155.

Menzies, N.W., Donn, M.J., Kopittke, P.M., 2007. Evaluation of extractants for estimation of the phytoavailable trace metals in soils. Environmental Pollution 145 (1), 121–130.

Merlot, S., La Garcia de Torre, V.S., Hanikenne, M., 2021. Physiology and Molecular Biology of Trace Element Hyperaccumulation, in: van der Ent, A., Baker, A.J., Echevarria, G., Simonnot, M.-O., Morel, J.L. (Eds.), Agromining: Farming for Metals. Mineral Resource Reviews. Springer International Publishing, Cham, pp. 155–181.

Mohseni, R., Ghaderian, S.M., Ghasemi, R., Schat, H., 2018. Differential effects of iron starvation and iron excess on nickel uptake kinetics in two Iranian nickel hyperaccumulators, Odontarrhena bracteata and Odontarrhena inflata. Plant Soil 428 (1), 153–162.

Montargès-Pelletier, E., Chardot, V., Echevarria, G., Michot, L.J., Bauer, A., Morel, J.-L., 2008. Identification of nickel chelators in three hyperaccumulating plants: An X-ray spectroscopic study. Phytochemistry 69 (8), 1695–1709.

Morrissey, J., Baxter, I.R., Lee, J., Li, L., Lahner, B., Grotz, N., Kaplan, J., Salt, D.E., Guerinot, M.L., 2009. The ferroportin metal efflux proteins function in iron and cobalt homeostasis in Arabidopsis. The Plant Cell 21 (10), 3326–3338.

Murphy, J., Riley, J.P., 1962. A modified single solution method for the determination of phosphate in natural waters. Analytica Chimica Acta 27, 31–36.

Mustafiz, A., Ghosh, A., Tripathi, A.K., Kaur, C., Ganguly, A.K., Bhavesh, A.K., Tripathi, J.K., Pareek, A., Sopory, S.K., Singla-Pareek, S.K., 2014. A unique Ni2+ -dependent and methylglyoxal-inducible rice glyoxalase I possesses a single active site and functions in abiotic stress response. The Plant journal : for cell and molecular biology 78 6, 951–963.

Nawara, S., van Dael, T., Merckx, R., Amery, F., Elsen, A., Odeurs, W., Vandendriessche, H., Mcgrath, S., Roisin, C., Jouany, C., Pellerin, S., Denoroy, P., Eichler-Löbermann, B., Börjesson, G., Goos, P., Akkermans, W., Smolders, E., 2017. A comparison of soil tests for available phosphorus in long-term field experiments in Europe. Eur J Soil Sci 68 (6), 873–885.

Nishida, S., Tsuzuki, C., Kato, A., Aisu, A., Yoshida, J., Mizuno, T., 2011. AtIRT1, the Primary Iron Uptake Transporter in the Root, Mediates Excess Nickel Accumulation in Arabidopsis thaliana. Plant Cell Physiol 52 (8), 1433–1442.

Olsen, S.R., 1954. Estimation of available phosphorus in soils by extraction with sodium bicarbonate 939. US Department of Agriculture.

ÖNorm L 1085, 2009. Chemische Bodenuntersuchungen: Extraktion von Elementen mit Königswasser oder Salpetersäure-Perchlorsäure-Gemisch. Österreichisches Normungsinstitut, Vienna, Austria.

ÖNorm L1086-89, 1989. Österreichische technische Norm: Chemical analysis of soils; determination of exchangeable cations and cation exchange capacity.

Oze, C., Fendorf, S., Bird, D.K., Coleman, R.G., 2004. Chromium Geochemistry of Serpentine Soils. International Geology Review 46 (2), 97–126.

Pardo, T., Rodríguez-Garrido, B., Saad, R.F., Soto-Vázquez, J.L., Loureiro-Viñas, M., Prieto-Fernández, Á., Echevarria, G., Benizri, E., Kidd, P.S., 2018. Assessing the agromining potential of Mediterranean nickel-hyperaccumulating plant species at field-scale in ultramafic soils under humid-temperate climate. Science of The Total Environment 630, 275–286.

Polacco, J.C., Mazzafera, P., Tezotto, T., 2013. Opinion – Nickel and urease in plants: Still many knowledge gaps. Plant Science 199-200, 79–90.

Proctor, J., Woodell, S.R., 1975. The Ecology of Serpentine Soils, in: MacFadyen, A. (Ed.), Advances in Ecological Research, vol. 9. Academic Press, pp. 255–366.

Puschenreiter, M., Schnepf, A., Millán, I.M., Fitz, W.J., Horak, O., Klepp, J., Schrefl, T., Lombi, E., Wenzel, W.W., 2005. Changes of Ni biogeochemistry in the rhizosphere of the hyperaccumulator Thlaspi goesingense. Plant Soil 271 (1-2), 205–218.

Puschenreiter, M., Wieczorek, S., Horak, O., Wenzel, W.W., 2003. Chemical changes in the rhizosphere of metal hyperaccumulator and excluder Thlaspi species. Journal of Plant Nutrition and Soil Science 166 (5), 579–584.

Puschenreiter, M., Wittstock, F., Friesl-Hanl, W., Wenzel, W.W., 2013. Predictability of the Zn and Cd phytoextraction efficiency of a Salix smithiana clone by DGT and conventional bioavailability assays. Plant Soil 369 (1), 531–541.

Rascio, N., Navari-Izzo, N., 2011. Heavy metal hyperaccumulating plants: How and why do they do it? And what makes them so interesting? Plant Science 180 (2), 169–181.

Ratié, G., Jouvin, D., Garnier, J., Rouxel, O., Miska, S., Guimarães, E., Cruz Vieira, L., Sivry, Y., Zelano, I., Montarges-Pelletier, E., Thil, F., Quantin, C., 2015. Nickel isotope fractionation during tropical weathering of ultramafic rocks. Chemical Geology 402, 68–76.

Reeves, R.D., 2003. Tropical hyperaccumulators of metals and their potential for phytoextraction. Plant Soil 249 (1), 57–65.

Reeves, R.D., Baker, A.J.M., Jaffré, T., Erskine, P.D., Echevarria, G., van der Ent, A., 2018. A global database for plants that hyperaccumulate metal and metalloid trace elements. The New phytologist 218 (2), 407–411.

Reeves, R.D., van der Ent, A., Echevarria, G., Isnard, S., Baker, A.J.M., 2021. Global Distribution and Ecology of Hyperaccumulator Plants, in: van der Ent, Antony and Baker, Alan J.M. and Echevarria, Guillaume and Simonnot, Marie-Odile and Morel, Jean Louis (Ed.), Agromining: Farming for Metals: Extracting Unconventional Resources Using Plants. Springer International Publishing, Cham, pp. 133–154.

Robinson, B.H., Brooks, R.R., Clothier, B.E., 1999. Soil Amendments Affecting Nickel and Cobalt Uptake by Berkheya coddii : Potential Use for Phytomining and Phytoremediation. Ann Bot 84 (6), 689–694.

Rosenkranz, T., Hipfinger, C., Ridard, C., Puschenreiter, M., 2019. A nickel phytomining field trial using Odontarrhena chalcidica and Noccaea goesingensis on an Austrian serpentine soil. Journal of environmental management 242, 522–528.

Schaaf, G., Honsbein, A., Meda, A.R., Kirchner, S., Wipf, D., Wirén, N. von, 2006. AtIREG2 Encodes a Tonoplast Transport Protein Involved in Iron-dependent Nickel Detoxification in Arabidopsis thaliana Roots*. Journal of Biological Chemistry 281 (35), 25532–25540.

Schoenau, J.J., O'Halloran, D.D., 2008. Sodium Bicarbonate-Extractable Phosphorus, in: Carter, M.R., Gregoric, E.G. (Eds.), Soil Sampling and Methods of Analysis 2. Taylor & Francis, pp. 89–94.

Shi, Z., Peltier, E., Sparks, D.L., 2012. Kinetics of Ni Sorption in Soils: Roles of Soil Organic Matter and Ni Precipitation. Environmental science & technology 46 (4), 2212–2219.

Španiel, S., Kempa, M., Salmerón-Sánchez, E., Fuertes-Aguilar, J., Mota, J.F., Al-Shehbaz, I.A., German, D.A., Olšavská, K., Šingliarová, B., Zozomová-Lihová, J., Marhold, K., 2015. AlyBase: database of names, chromosome numbers, and ploidy levels of Alysseae (Brassicaceae), with a new generic concept of the tribe. Plant Systematics and Evolution 301 (10), 2463–2491.

Taylor, S.I., Macnair, M.R., 2006. Within and between population variation for zinc and nickel accumulation in two species of Thlaspi (Brassicaceae). The New phytologist 169 (3), 505–513.

Tognacchini, A., Rosenkranz, T., van der Ent, A., Machinet, G.E., Echevarria, G., Puschenreiter, M., 2020. Nickel phytomining from industrial wastes: Growing nickel hyperaccumulator plants on galvanic sludges. Journal of environmental management 254, 109798.

U.S. Geological Survey, 2022. Nickel - Mineral Commodity Summaries: January 2022. https://pubs.usgs.gov/periodicals/mcs2022/mcs2022-nickel.pdf. Accessed 16 June 2022.

van der Ent, A., Baker, A.J.M., Reeves, R.D., Chaney, R.L., Anderson, C.W.N., Meech, J.A., Erskine, P.D., Simonnot, M.-O., Vaughan, J., Morel, J.L., Echevarria, G., Fogliani, B., Rongliang, Q., Mulligan, D.R., 2015. Agromining: Farming for Metals in the Future? Environmental science & technology 49 (8), 4773–4780.

van der Ent, A., Baker, A.J.M., Reeves, R.D., Pollard, A.J., Schat, H., 2013. Hyperaccumulators of metal and metalloid trace elements: facts and fiction. Plant Soil 362 (1), 319–334.

van der Ent, A., Cardace, D., Tibbett, M., Echevarria, G., 2018. Ecological implications of pedogenesis and geochemistry of ultramafic soils in Kinabalu Park (Malaysia). Catena 160, 154–169.

van der Ent, A., Echevarria, G., Tibbett, M., 2016. Delimiting soil chemistry thresholds for nickel hyperaccumulator plants in Sabah (Malaysia). Chemoecology 26 (2), 67–82.

van der Pas, L., Ingle, R.A., 2019. Towards an Understanding of the Molecular Basis of Nickel Hyperaccumulation in Plants. Plants (Basel, Switzerland) 8 (1).

Verbruggen, N., Hermans, C., Schat, H., 2008. Molecular mechanisms of metal hyperaccumulation in plants. The New phytologist 181 (4), 759–776.

Waldstein-Wartenberg, F.A. von, Kitaibel, P., 1799. Descriptiones et icones plantarum rariorum Hungariae. Vol. 1. M.A. Schmidt, Vienna.

Wenzel, W.W., Bunkowski, M., Puschenreiter, M., Horak, O., 2003. Rhizosphere characteristics of indigenously growing nickel hyperaccumulator and excluder plants on serpentine soil. Environmental Pollution 123 (1), 131–138.

Wenzel, W.W., Kidd, P.S., Puschenreiter, M., Rosenkranz, T., 2018. Nickel Biogeochemistry at the Soil–Plant Interface. In: Nickel in Soils and Plants; Tsadilas, C., Rinklebe, J., Selim, M., Eds, 21–50.

Wenzel, W.W., Lombi, E., Adriano, D.C., 2004. Root and Rhizosphere Processes in Metal Hyperaccumulation and Phytoremediation Technology, in: Prasad, M.N.V. (Ed.), Heavy Metal Stress in Plants: From Biomolecules to Ecosystems. Springer Berlin Heidelberg, Berlin, Heidelberg, pp. 313–344.

Wicks, F.J., O'Hanley, D.S., 1988. Chapter 5. SERPENTINE MINERALS: STRUCTURES AND PETROLOGY, in: S. W. Bailey (Ed.), Hydrous Phyllosilicates: (Exclusive of Micas). De Gruyter, pp. 91–168.

Yada, K., 1967. Study of chrysotile asbestos by a high resolution electron microscope. Acta Cryst 23 (5), 704–707.

Yariv, S., Heller-Kallai, L., 1975. The Relationship between the I.R. Spectra of Serpentines and Their Structures. Clays and Clay Minerals 23 (2), 145–152.

York, L.M., Carminati, A., Mooney, S.J., Ritz, K., Bennett, M.J., 2016. The holistic rhizosphere: integrating zones, processes, and semantics in the soil influenced by roots. Journal of experimental botany 67 (12), 3629–3643.

10 Supplementary Material

Table 5: Dry weight of O. chalcidica divided into shoots and roots. Concentration of elements in shoots of O. chalcidica in mg kg of DW and in µg of Ni per plant biomass (DW). Average values (n = 4) ± standard deviation, DW = dry weight.

	soil 1	soil 2	soil 3	soil 4	soil 5	soil 6	soil LS
	mg DW	mg DW	mg DW	mg DW	mg DW	mg DW	mg DW
Biomass							
Shoots	477 ± 112	581 ± 8.5	552 ± 72	577 ± 181	606 ± 133	946 ± 183	773 ± 41
Roots	349 ± 91	297 ± 41	308 ± 115	306 ± 113	317 ± 99	385 ± 95	334 ± 32
	mg kg^{-1}	mg kg^{-1}	mg kg^{-1}	mg kg^{-1}	mg kg^{-1}	mg kg^{-1}	mg kg^{-1}
Conc. in shoots							
Ni	2442 ± 547	3873 ± 814	5787 ± 1072	4080 ± 1670	4780 ± 1595	7667 ± 759	7514 ± 759
Fe	56 ± 4.3	59 ± 11	62 ± 10	60 ± 14	49 ± 10	48 ± 3.1	41 ± 6.8
K	9373 ± 1967	8061 ± 1301	8529 ± 2011	8220 ± 2678	6763 ± 2638	5990 ± 651	8911 ± 670
P	570 ± 89	542 ± 28	651 ± 150	609 ± 122	605 ± 77	594 ± 3.3	900 ± 58
Zn	152 ± 62	142 ± 28	126 ± 16	78 ± 17	81 ± 23	102 ± 15	62 ± 10
Mg	5235 ± 541	5485 ± 902	6000 ± 744	6507 ± 605	5484 ± 783	4683 ± 1056	2880 ± 620
Ca	9020 ± 1517	8268 ± 1325	7821 ± 1761	8583 ± 1084	8425 ± 2084	7153 ± 1531	14664 ± 5192
S	1396 ± 163	1223 ± 30	1246 ± 153	1270 ± 198	1209 ± 253	931 ± 67	2509 ± 441
Mn	116 ± 20	92 ± 20	61 ± 17	45 ± 4.0	35 ± 10	42 ± 7.4	45 ± 10
	µg $plant^{-1}$ DW	µg $plant^{-1}$ DW	µg $plant^{-1}$ DW	µg $plant^{-1}$ DW	µg $plant^{-1}$ DW	µg $plant^{-1}$ DW	µg $plant^{-1}$ DW
Ni	1125 ± 134	2246 ± 460	3249 ± 777	2386 ± 965	2985 ± 1440	7277 ± 1784	5808 ± 675

Table 6: Chemical characterisation of the experimental soils after the pot experiment. DTPA extractable metals, bioavailable Olsen-P, $Sr(NO_3)_2$ extractable metals and soil pH (in H_2O) of soils. Values are averaged (n = 4) ± standard deviation. LOQ = Limit of quantification.

	Soil 1		Soil 2		Soil 3		Soil 4		Soil 5		Soil 6		Soil LS	
	planted	control	planted	control	planted	control	planted	control	planted	control	planted	control	planted	control
	mg kg $^{-1}$		mg kg $^{-1}$		mg kg $^{-1}$		mg kg $^{-1}$		mg kg $^{-1}$		mg kg $^{-1}$		mg kg $^{-1}$	
DTPA														
Ni	40.9 ± 3.6	47.7 ± 2.4	62.4 ± 2.1	71.1 ± 2.8	83.6 ± 4.1	101 ± 4.5	124 ± 6.4	132 ± 3.5	145 ± 10.1	161 ± 4.5	157 ± 16	188 ± 7.9	55.9 ± 0.4	61.1 ± 2.5
Fe	419 ± 49	387 ± 18	397 ± 23	363 ± 40	364 ± 62	363 ± 32	434 ± 20	404 ± 23	379 ± 16	377 ± 8.2	352 ± 14	337 ± 15	46.8 ± 3.1	40.9 ± 4.5
Mn	21.8 ± 2.3	22.9 ± 1.5	24.2 ± 1.4	23.9 ± 3.2	23.6 ± 4.4	27.7 ± 4.6	28.2 ± 1.4	28.0 ± 0.4	27.5 ± 1.0	28.0 ± 1.5	29.4 ± 1.8	28.9 ± 1.0	8.12 ± 0.2	7.30 ± 0.8
Co	1.58 ± 0.2	1.72 ± 0.1	1.82 ± 0.1	1.82 ± 0.3	1.87 ± 0.4	2.18 ± 0.4	2.37 ± 0.1	2.35 ± 0.1	2.30 ± 0.1	2.35 ± 0.1	2.41 ± 0.2	2.45 ± 0.1	0.65 ± 0.01	0.59 ± 0.1
Cu	1.32 ± 0.2	1.17 ± 0.2	1.48 ± 0.1	1.42 ± 0.1	1.68 ± 0.2	1.76 ± 0.2	2.40 ± 0.1	2.28 ± 0.2	2.67 ± 0.1	2.62 ± 0.1	3.00 ± 0.1	2.92 ± 0.1	2.27 ± 0.1	2.22 ± 0.1
Zn	3.20 ± 0.3	3.37 ± 0.2	2.64 ± 0.1	2.65 ± 0.2	2.27 ± 0.3	2.37 ± 0.2	2.33 ± 0.3	2.18 ± 0.1	1.85 ± 0.2	2.09 ± 0.4	1.78 ± 0.1	1.95 ± 0.1	0.33 ± 0.1	0.38 ± 0.2
Olsen-P	7.84 ± 1.5	8.05 ± 2.0	7.68 ± 1.3	7.59 ± 2.2	6.97 ± 1.0	7.97 ± 0.3	7.43 ± 0.6	6.73 ± 0.5	6.43 ± 1.1	7.60 ± 0.6	6.82 ± 0.6	7.08 ± 0.4	1.81 ± 0.2	2.60 ± 0.2
	µg kg $^{-1}$		µg kg $^{-1}$		µg kg $^{-1}$		µg kg $^{-1}$		µg kg $^{-1}$		µg kg $^{-1}$		µg kg $^{-1}$	
$Sr(NO_3)_2$														
Ni	672 ± 40	835 ± 26	853 ± 32	1107 ± 44	968 ± 45	1302 ± 47	1102 ± 87	1358 ± 32	1144 ± 75	1377 ± 11	967 ± 59	1389 ± 27	299 ± 18	337 ± 17
Fe	109 ± 28	76.8 ± 29	96.1 ± 8.3	72.3 ± 22	94.6 ± 40	77.3 ± 20	127 ± 13	127 ± 18	118 ± 14	103 ± 8.6	132 ± 55	118 ± 29	54.0 ± 52	42.3 ± 43
Mn	1328 ± 406	1481 ± 454	1382 ± 245	1382 ± 615	920 ± 519	1510 ± 558	1081 ± 52	1285 ± 92	907 ± 11	1028 ± 49	737 ± 32	870 ± 31	70.6 ± 20	62.2 ± 13
Co	43.8 ± 9.8	49.1 ± 12	42.9 ± 6.2	45.0 ± 17	29.5 ± 13	46.5 ± 15	32.8 ± 2.2	38.3 ± 2.6	27.0 ± 0.7	30.6 ± 1.1	20.8 ± 1.3	24.8 ± 0.8	4.09 ± 1.4	3.10 ± 0.3
Cu	22.3 ± 0.6	27.0 ± 8.8	19.8 ± 5.7	18.8 ± 1.3	16.7 ± 4.3	14.8 ± 4.9	10.8 ± 2.1	15.2 ± 4.3	11.5 ± 1.4	18.0 ± 3.7	12.1 ± 3.3	12.5 ± 3.7	< LOQ	< LOQ
Zn	109 ± 3.5	120 ± 4.2	88.9 ± 9.4	100 ± 17	69.9 ± 6.2	74.9 ± 3.4	54.9 ± 2.9	62.9 ± 7.7	64.3 ± 26	56.5 ± 5.9	44.3 ± 1.0	49.9 ± 4.0	37.5 ± 3.5	42.3 ± 4.7
	[-]		[-]		[-]		[-]		[-]		[-]		[-]	
pH	5.90 ± 0.04	5.66 ± 0.04	6.02 ± 0.03	5.78 ± 0.03	6.10 ± 0.1	5.84 ± 0.04	6.19 ± 0.1	6.00 ± 0.02	6.28 ± 0.1	6.09 ± 0.1	6.54 ± 0.03	6.18 ± 0.04	8.02 ± 0.02	7.99 ± 0.04

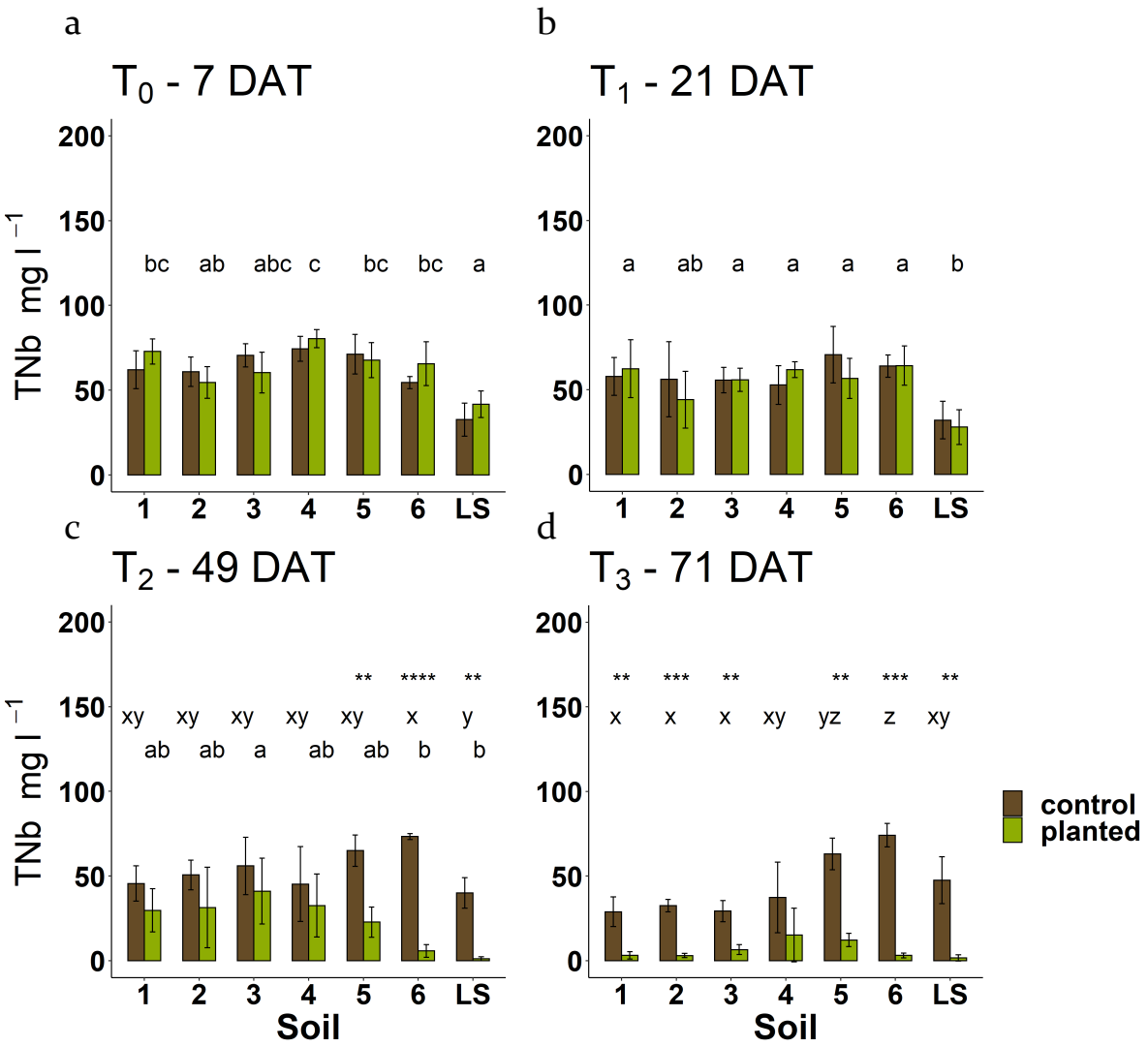

Figure 18: Total N concentrations of pore water samplings T0 to T3 of planted (green) and unplanted (brown) pots. Average values (n = 4) ± standard deviation, asterisks: p < 0.05 "", p < 0.01 "**", p < 0.001 "***", p < 0.0001 "****" indicate significance between planted and control pots of the same soil, letters "abc" indicate significance between planted pots and "xyz" between control pots, p < 0.05. DAT = days after transplantation of seedlings into the pot experiment.*